New insights into the structure of the South Caspian Basin from seismic reflection data, Gorgan Plain, Iran

Ali Radfar, Aziz Rahimi Chakdel, Ali Nejati, Mehrdad Soleimani & FaridTaati

International Journal of Earth Sciences
GR Geologische Rundschau

ISSN 1437-3254

Int J Earth Sci (Geol Rundsch)
DOI 10.1007/s00531-018-1659-x

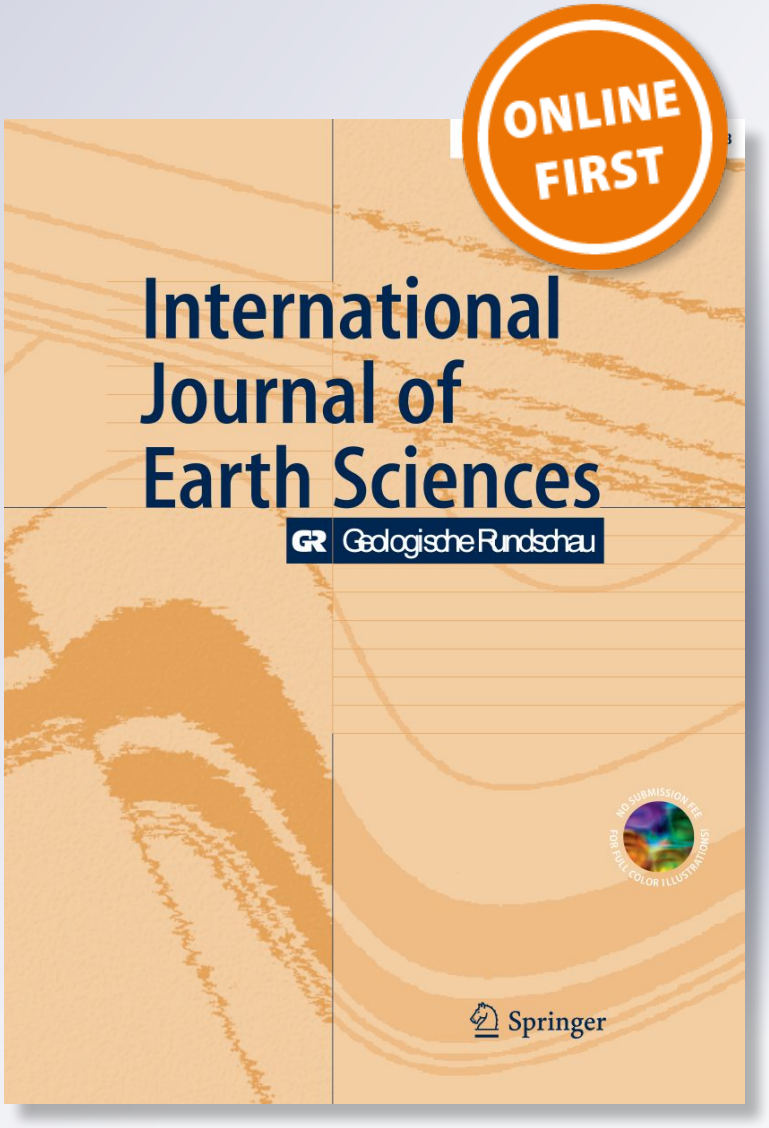

Springer

International Journal of Earth Sciences
https://doi.org/10.1007/s00531-018-1659-x

ORIGINAL PAPER

New insights into the structure of the South Caspian Basin from seismic reflection data, Gorgan Plain, Iran

Ali Radfar[1] · Aziz Rahimi Chakdel[1] · Ali Nejati[2] · Mehrdad Soleimani[2] · FaridTaati[3]

Received: 13 March 2018 / Accepted: 24 October 2018

Abstract

This research presents an integrated study of 2D seismic reflections and calibrated well data to outline the structural development of the Gorgan Plain on the border of the South Caspian hydrocarbon basin, in the Alborz and Kopeh-dagh ranges of northeast Iran. Eight seismic horizons, including two unconformities, have been identified, ranging in age from Early Jurassic to Quaternary. Analysis and interpretation of geophysical data provide an understanding of the structural geology of the Gorgan Plain, crucial for investigation of structural traps. Seismic interpretation indicates structural features such as deep reverse listric faults (inverted normal faults) for older formations; strike-slip and normal faults in younger sequences; dome and basin interference patterns of folding for all the top formations. Well data demonstrate the occurrence of a disconformity at the base of Upper Cretaceous beds and an angular unconformity at the base of Paleogene. Evidence identified in well and seismic-reflection data proves a complex pattern of tectonic phases since the Early Jurassic. It seems reasonable to suppose that these structural patterns are related to a change in direction of tectonic compression, which in turn has produced structural hydrocarbon traps in crests of domes in the Gorgan area.

Keywords Gorgan plain · South Caspian Basin · Alborz range · 2D seismics · Two-way-time map · Hydrocarbon traps

Introduction

The Gorgan Plain is located in the Golestan province on the southeastern coast of the Caspian Sea (N–NE Iran) (Fig. 1). From a geological point of view, the Golestan province is bordered by three different geological zones. It lies mostly in the southern part of the South Caspian Basin (hereafter SCB) bounded by the Alborz ranges (hereafter Alborz) to the south and the Kopeh-Dagh mountains (hereafter KDM) to the east (Fig. 2).

The Gorgan Plain is covered by a thick sequence of Quaternary sediments without any exposure of the bedrocks, and the authors had arguments about the affinity of this region to the SCB or KDM over many years. Because of lack of surface structural data in the Gorgan Plain, the authors endeavored to collect data from geophysical methods (especially seismic reflection) and well logging to model subsurface structures. Structural modeling of the region is a key step to determine the geologic history and geodynamic setting of the Gorgan Plain. Hydrocarbon production has an important role in the economy of the countries around the SCB, especially Azerbaijan and Turkmenistan. Many scientific researches have been done and published in this geological zone (e.g., Narimanov 1993; Abrams and Narimanov 1997; Bagirov et al. 1997; Efendiyeva 2000; Katz et al. 2000; Buryakovsky et al. 2001; Diaconescu et al. 2001; Ulmishek 2001; Guliyev et al. 2003; Tolosa et al. 2004; Smith-Rouch 2006; Alizada et al. 2014; Gorodnitskiy et al. 2013). Many hydrocarbon fields are active in the Turkmenistan part of the SCB and KDM (Robert et al. 2014; Smith-Rouch 2006). Unfortunately, sufficiently comprehensive studies on exploration and production of hydrocarbons in the Iranian part of the SCB have not been implemented so far. Exploration and extraction of hydrocarbon materials from both SCB and KDM demonstrated that the Gorgan Plain also has potential hydrocarbon generation.

✉ Aziz Rahimi Chakdel
a.rahimi@gu.ac.ir

[1] Department of Geology, Faculty of Science, Golestan University, Shahid Beheshti Street, 49138-15759 Gorgan, Iran

[2] Faculty of Mining, Petroleum and Geophysics, Shahrood University of technology, 7th Tir Square, Shahrood, Iran

[3] Khazar Exploration and Production Company (KEPCO), NO. 19, 11th Alley, Vozara Street, Tehran, Iran

Published online: 09 November 2018

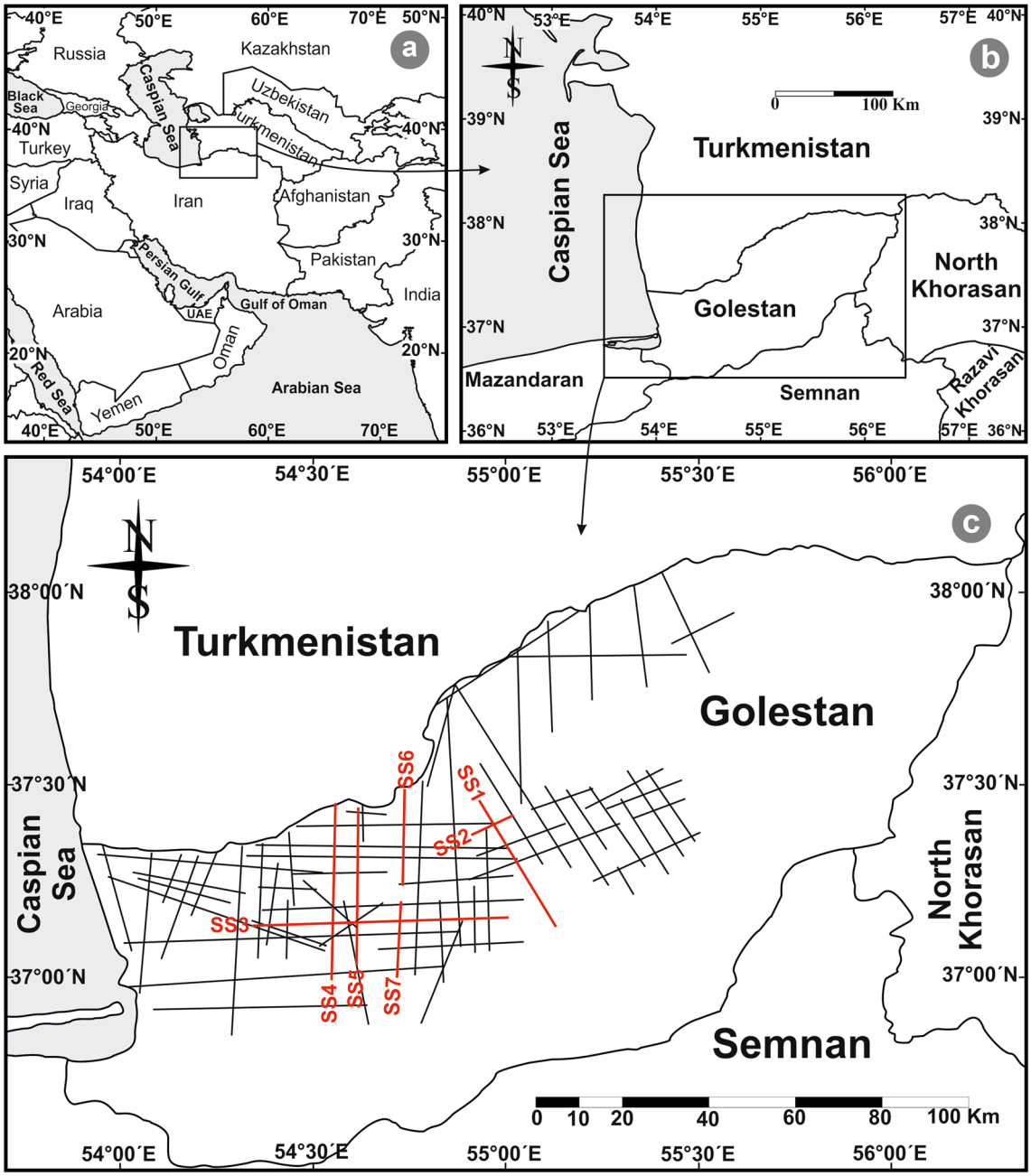

Fig. 1 The geographical location of the study area, **a** location of Iran in the Middle East, **b** Golestan province at the southeastern boundary of the Caspian Sea, and **c** seismic profiles collected from the Gorgan Plain. Note that the red lines are used for this study

Rad (1982, 1986) studied the hydrocarbon potential of the Shemshak Group in the Eastern Alborz. He suggested that deposition of the Shemshak Formation took place in a rapid subsiding deltaic environment at the border of Tethys Ocean. Also he concluded that although the hydrocarbon generation potential of the Shemshak Group is low, under favorable conditions this formation is capable of becoming a giant oil and gas field. Narimanov (1993) surveyed the characteristics of SCB hydrocarbon traps and pointed out that most hydrocarbons of the basin are found in a variety of structural traps formed during Late Pliocene folding of Early Pliocene age. During Late Pliocene, an increase of tectonic activities caused folding of the underlying formations. This folding event led to the development of structural traps (Narimanov 1993). Alavi (1996), based upon lithologic, structural and stratigraphic analyses of the exposed rocks in the Alborz, introduced seven tectono-stratigraphic units and expressed Alborz as a composite antiformal stack

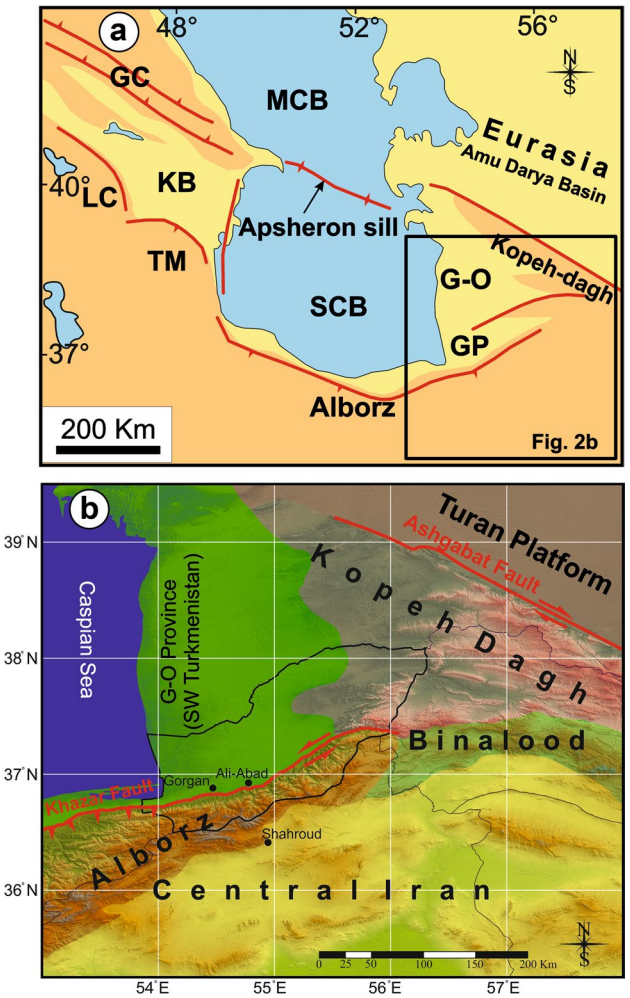

Fig. 2 **a** Structural and tectonic setting of the South Caspian Basin and the location of surrounding structural features (slightly modified after Stewart and Davis 2006). GC, Greater Caucasus Mountain; LC, Lesser Caucasus Mountain; TM, Talesh Mountain; KB, Kura Basin; SCB, South Caspian Basin; MCB, Middle Caspian Basin; GP, Gorgan Plain; G-O, Gograndag-Okarem Province (Southwestern Turkmenistan). **b** Tectonic setting and zonation of the study area and adjacent places at the south and east of South Caspian Basin

formed during Cimmerian and Alpine Orogenies. Jackson et al. (2002) studied the active tectonics of the SCB. Based on the lack of earthquakes within the SCB and depth of earthquakes in surrounding areas (~30 km in Alborz, KDM and Talesh; and ~80 km in Apsheron–Balkhan sill), they claimed that the SCB has started to subduct beneath the Central Caspian since Pliocene time. They also estimated the westward motion of SCB relative to Iran (13–17 mm/year to SW) and Eurasia (8–10 mm/year to NW). Using geodetic data, Vernant et al. (2004) measured the amount of deformation through Alborz during Cenozoic. They explained that the deformation of Central Alborz represents 40% (~5 mm/year) of shortening between Central Iran and Eurasia. They interpreted their results as follows: the remaining shortening should occur in the SCB (~6 mm/year) and northern edge of Central Iranian Block (~3 mm/year). Knapp et al. (2004) studied the crustal-scale seismic-reflection data of SCB in the vicinity of the Apsheron (or Absheron) Ridge (offshore Azerbaijan) and analyzed the properties of oceanic crust and sedimentary fill of the SCB. They also presented compelling evidence for the northward subduction of the South Caspian oceanic lithosphere beneath the continental lithosphere of Central Caspian Basin (southern margin of Eurasia). Torres (2007) presumed that hydrocarbon traps of the Gograndag Okarem province (the eastern border of SCB in Turkmenistan) appear to be as structural types which continued into the Gorgan Plain. There is current production of hydrocarbons from KDM and the eastern limb of the SCB (Robert et al. 2014) in Turkmenistan (Torres 2007) and Kazakhstan (Ulmishek 2001). According to the above evidence, geographical location and geologic resemblance of the Gorgan Plain (at the north of the Alborz range) to the Gograndag-Okarem step of Turkmenistan, it is reasonably conceivable that the area has hydrocarbon reservoir potential. Kadirov and Gadirov (2014) developed a 2D gravity model and investigated crustal structure variations of the SCB by using a combination of geological and geophysical data, including deep 2D seismic-reflection data. They provided evidence for subduction of South Caspian oceanic crust under the Central Caspian continental lithosphere, and suggested that the subduction has started recently and the subducting slab has not yet reached the mantle to activate volcanism.

Understanding of the geological and structural evolution of the Gorgan Plain is thought to be essential for building a predictive geological model for prospection of petroleum traps in the region. The key to success in building an accurate geological model is through integration of geophysical and geological data. In this study, seven 2D reflection seismic images are interpreted and the results integrated with a field-based geological model to produce an improved structural model of the Gorgan Plain relevant to any future petroleum exploration studies.

Geologic background

The study area straddles three geological zones (SCB, KDM and Alborz), which are briefly outlined below.

The Alborz is an intra-continental orogen located between the SCB and Central Iran (Allen et al. 2004) (Fig. 2). It is still active due to both the northward movement of Central Iran and northwestward movement of the SCB with respect to Eurasia (Ritz et al. 2006; Nabavi et al. 2017). From the structural point of view, Alborz is a double-verging reverse and sub-vertical strike-slip fault system that extends parallel to the Caspian shore line from Azerbaijan to Afghanistan (Ballato et al. 2011, 2013; Nabavi et al. 2017). The Alborz

Mountains are bordered by the SCB to the north, Central Iran to the south, the lesser Caucasus to the west, and the Paropamisus mountains to the east (Alavi 1996). Precambrian crystalline basement is only exposed within the range at one site in the Lahijan Granite at the western part of belt (Allen et al. 2004; Zanchi et al. 2009). The stratigraphy of this zone is characterized by dominance of platform-type sediments including limestone, dolostone and clastic rocks that range in age from Precambrian to Quaternary with some hiatus in the Paleozoic and Mesozoic (Ghorbani 2013). The Alborz range belonged to Gondwana land during the Paleozoic. During the Permian, Alborz started to separate from Gondwana and drifted toward Eurasia (Fürsich et al. 2009a). From the Precambrian to Middle Triassic, sedimentary successions of the Alborz were affected by opening of the Paleotethys Ocean and Neotethys Ocean during the Early Paleozoic and Late Paleozoic times, respectively (Stampfli et al. 1991). Therefore, the Alborz acted probably as a passive margin during these times. During the Late Triassic, the separated Alborz block collided with Eurasia causing the Eo-Cimmerian orogeny (Allen et al. 2003a; Berra et al. 2007; Golonka 2007; Zanchi et al. 2009; Nabavi et al. 2017). The Precambrian to Middle Triassic successions were deformed during the Eo-Cimmerian orogeny and uplifted and eroded before being unconformably overlain by terrigenous successions of the Shemshak Group (Late Triassic–Middle Jurassic) (Berra et al. 2007; Golonka 2007; Zanchi et al. 2009). Subsequently, platform-type limestones covered the above successions by an unconformity, indicating that the Alborz experienced the Mid-Cimmerian tectonic event during Jurassic (Fürsich et al. 2009a). The Jurassic–Cretaceous carbonates were unconformably covered by Paleocene–Eocene carbonates, volcanic and volcaniclastic complexes (Allen et al. 2003a; Zanchi et al. 2006). The coastal terrigenous units with evaporites and limestones (Miocene) are overlain by the Plio-Quaternary clastic sediments in the Alborz Basin (Zanchi et al. 2006).

The Kopeh-Dagh Mountain (KDM) This structural zone is about 600 km long and located along the border of Iran and Turkmenistan in northern Central Iran. This zone is limited to the west by the Caspian Sea and the Alborz mountain chain, to the south by Central Iran block, and to the north and northeast by the Eurasian Amu Darya Basin by the right-lateral strike-slip Ashgabat fault (Fig. 2). The tectonics of this area have received less attention than other zones in the region (the Zagros, the Alborz and the Central Iran), so the tectonic evolution of KDM is not completely understood (Hollingsworth et al. 2006; Bretis et al. 2012). Formations of the KDM are relatively younger than those of the Alborz (Hollingsworth et al. 2006). The oldest rocks exposed in the KDM are within the Aghdarband erosional window (Devonian–Carboniferous metasediments) (Zanchi et al. 2016 and references therein) and within Fariman–Darreh Anjir complexes (Permian) (Zanchetta et al. 2013 and references therein). These Paleozoic formations with the Triassic successions of the KDM were severely deformed during the Eo-cimmerian orogeny and were unconformably covered by the Middle Jurassic Kashafrud Formation (Taheri et al. 2009; Zanchetta et al. 2013; Zanchi et al. 2016). The Kopeh-dagh and Amu Darya basins started to open between Central Iran and Eurasia during Early Jurassic times allowing marine sedimentation to occur (Bretis et al. 2012). Convergence between the Turan platform of Eurasia and Central Iran commenced in Late Cretaceous–Paleocene times (Hollingsworth et al. 2006; Bretis et al. 2012) leaving a shallow marine sea in the north of KDM and erosion of the Alborz leading to deposition of continental red-bed sediments in the KDM (Hollingsworth et al. 2006, 2010). The time span during which the uplift of the KDM occurred was estimated to vary from Oligocene to Pliocene–Quaternary (Hollingsworth et al. 2006).

The South Caspian Basin (SCB) This zone is bounded to the north by the Apsheron sill, to the south by the Alborz, to the west by the Talesh Mountains and the Kura Basin, and to the east by the Kopeh-dagh fold and thrust belt (Fig. 2). The SCB is a remnant of a back-arc basin in the north of a Neo-Tethyan arc (Allen et al. 2003a; Brunet et al. 2003) which was developed near the Greater Caucasus Mountains during Paleogene (Diaconescu et al. 2001). According to geophysical data and gravimetric modeling, the basement of the SCB is an oceanic (basaltic) crust with a thickness of about 15 km at the eastern part of the South Caspian Sea (Brunet et al. 2003) overlain by 20–25 km of Cretaceous–Quaternary sedimentary fill (Abrams and Narimanov 1997; Allen et al. 2003a; Brunet et al. 2003; Smith-Rouch 2006).

The ~ 10 km-thick Pliocene–Quaternary part of this succession was deposited in a 5.5 Myr interval (against 800 m of sediments in the northern flank of the Alborz) indicating rapid subsidence rate for the SCB (Mousavi-Ruhbakhsh 2001; Allen et al. 2003a). Several authors argued about the oldest strata appearance in the SCB. Some believe that deposition of sediment in the SCB started in the Callovian–Late Jurassic (Brunet et al. 2003, 2007; Torres 2007) with the fast deposition rate being in the Pliocene and Quaternary, while others believe that the oldest deposits found in the SCB are the Maykop suite which is considered to be of Oligo-Miocene age (Jackson et al. 2002; Allen et al. 2003a). The Maykop suite is the major hydrocarbon source rock of the SCB (Abrams and Narimanov 1997; Jackson et al. 2002). This suite is overlain by Upper Miocene evaporites. At the interval between Miocene and Pliocene, thick layers of productive series were deposited upon the old layers and formed the main hydrocarbon reservoir of the basin (Jackson et al. 2002; Allen et al. 2003a; Smith-Rouch 2006). The Pliocene sequence in the SCB consists of the Cheleken suite (Early Pliocene) and the Akchgyl suite (Late Pliocene). The

Quaternary succession in the SCB are made of the Apsheron Formation, Ancient Caspian Formation which itself divides into three subzones (Baku, Khazarian and Khovalynskian), and finally Novocaspian (Neocaspian) Formation (Mousavi-Ruhbakhsh 2001).

The overall geodynamic setting involves a rapid subsiding of the SCB surrounded by the Alborz and the KDM in the south and east, respectively. The rapid subsidence of the SCB was simultaneous with uplifting of the Alborz and the KDM in the Pliocene–Quaternary period.

Tectonic setting

The geology of the region is related to the convergence of the Arabian and Eurasian plates that started in Eo-cimmerian and continues up to present time (e.g., Stöcklin 1968; Berberian and King 1981; Jackson et al. 2002; McQuarrie et al. 2003; Allen et al. 2003a, 2004, 2006; Vernant et al. 2004; Ritz et al. 2006; Zanchi et al. 2006, 2016; Hollingsworth et al. 2006, 2010; Ballato et al. 2011; Zanchetta et al. 2013; Robert et al. 2014; Mattei et al. 2015, 2017). In fact, this region experienced two major compressional events similar to the other parts of Iranian Plateau. Both of these tectonic events are related to the convergence of the Gondwanan-derived terranes and the Eurasia (Robert et al. 2014). The first event occurred during the closure of the Paleotethys Ocean which caused the Cimmerian orogeny. The second event also took place during the closure of the Neotethys Ocean which brought about the Late Eocene compressional stresses (Vincent et al. 2005; Allen and Armstrong 2008; Rezaeian et al. 2012). Palaeomagnetic evidence suggests that the Iranian block(s) was (were) located at the northern margin of the Gondwanaland in Paleozoic and remained in this position until the Late Permian–Early Triassic when the Cimmerian blocks (including Central Iran, Afghanistan, Karakoram and Qiangtang) drifted from Gondwana and started to migrate toward Eurasia (Guest et al. 2006b; Muttoni et al. 2009a, b; Mattei et al. 2015), leading to the northward subduction of the Paleotethys Ocean beneath the Eurasia. The Neotethys Ocean opened to the south of the Central Iranian block (Guest et al. 2006a, b; Muttoni et al. 2009a, b). The closure of Paleotethys (collision of the Central Iranian microcontinent to the southern margin of Eurasia) happened in Late Triassic–Early Jurassic time, resulting in the Eo-cimmerian orogeny (Berberian and King 1981; Guest et al. 2006a, b; Muttoni et al. 2009a; Zanchi et al. 2009, 2016; Hollingsworth et al. 2010; Zanchetta et al. 2013; Berra and Angiolini 2014; Robert et al. 2014; Mattei et al. 2015, 2017). The Late Triassic–Early Jurassic collision suture zone lies along the northern margin of the Alborz and southern boundary of the KDM (Stöcklin 1974; Berberian and King 1981; Berberian 1983; Alavi 1996; Brunet et al. 2003; Guest et al. 2006b; Hollingsworth et al. 2010; Robert et al. 2014) (Fig. 2). After the Late Triassic–Early Jurassic collision, the subduction migrated southward of the Cimmerian blocks and a northward subduction started at the northern margin of Neotethys (Brunet et al. 2003). The long-lived northward subduction of Neotethyan oceanic crust formed a post-orogenic rift basin in north of the Paleotethys suture zone and the Greater Caucasus–Caspian back-arc basin was opened at the beginning of Middle Jurassic (Brunet et al. 2003; Golonka 2007; Taheri et al. 2009; Poursoltani and Gibling 2011; Robert et al. 2014). The eastern part of this back-arc basin was the origin of the SCB (Brunet et al. 2003; Golonka 2007). The absence of the Lower Jurassic sediments provides evidence for a period of emergence in south of the Turan platform (southern margin of Eurasia) (Lyberis et al. 1998). Thereafter, the Central Iranian microcontinent was encircled by small oceanic basins (branches of Neotethys) and became temporarily separated from Eurasia during the end of Jurassic–Early Cretaceous time (Stöcklin 1974; Hollingsworth et al. 2010; Mattei et al. 2015). During Late Cretaceous–Early Paleocene, the northward motion of the Afro-Arabian plate caused: (1) shortening along the northern margin of Neotethys; (2) closure of the aforesaid small oceanic basins; (3) re-collision of the Central Iranian microcontinent to the Eurasia (Hollingsworth et al. 2010; Mattei et al. 2015). Afterward, northward subduction of the Neotethys oceanic crust continued due to the northward movement of the Afro-Arabian plate, and the Arabia–Eurasia collision took place during the Late Eocene–Oligocene (Allen and Armstrong 2008; Hollingsworth et al. 2010; Allen et al. 2011; Rezaeian et al. 2012). The Alborz and KDM started to uplift due to the Arabia–Eurasia collision during the Oligo-Miocene (Axen et al. 2001; Brunet et al. 2003; Allen et al. 2004; Guest et al. 2006a, b; Hollingsworth et al. 2010). But the major deformation of this compressional event is manifested by lengthening of the Iranian crust in southeast direction. This lengthening happened because of a free face at the eastern side of the Arabia–Eurasia collision zone (Allen et al. 2011). The lengthening in SE direction continued until the Pliocene, when the Afghan–India collision occurred in the eastern side of the Arabia–Eurasia suture zone (Allen et al. 2011; Rezaeian et al. 2012). After the Afghan–India collision, the continuing convergence of Arabia and Eurasia caused the reorganization of tectonic regime, acceleration of the uplift and deformation of the Alborz and KDM in Pliocene (Brunet et al. 2003; Allen et al. 2004, 2011; Allen and Armstrong 2008; Reazeian et al. 2012).

Stratigraphic description

The area is entirely covered by Quaternary sediments with no surface exposure of bedrocks (Fig. 3). The stratigraphy described here is thus based on geologic data obtained from four drilled wells in the Gorgan Plain (Figs. 4, 5).

Kashafrud Formation (Late Bajocian–Bathonian)

This is the oldest formation observed in the W2 well (see Sect. 4.2; Table 2) which penetrated about 70 m into the Kashafrud Formation (see Table 2; Fig. 4). This unit consists of black micaceous shale and alternation of black quartz-bearing shale with calcareous sandstone. In the type section, the Middle Jurassic Kashafrud Formation unconformably overlies folded Triassic and/or older rocks in this subsiding post-orogenic rift basin (Kavoosi et al. 2009; Taheri et al. 2009; Poursoltani and Gibling 2011; Robert et al. 2014; Zanchi et al. 2016) and includes at least 300–3000 m of deep marine siliciclastic sediments ranging from conglomerates to clays whose provenance are from the Binalood Mountain (eastern prolongation of the Alborz) (Taheri et al. 2009). It was deposited in Late Bajocian–Bathonian times (Kavoosi et al. 2009; Poursoltani and Gibling 2011) (Fig. 4). Following the collision of Cimmerian terranes to the southern margin of Eurasia, a post-orogenic rift system extended and the Kashafrud Basin was opened in the north of Paleotethys suture zone (Taheri et al. 2009). This post-orogenic subsiding basin was the eastern prolongation of the SCB (Brunet et al. 2003; Taheri et al. 2009). This formation shows abrupt thickening zones from Turkmenistan toward Iran. These zones of abrupt thickening are inferred to mark extensional faults during deposition of the Kashafrud Formation (Kavoosi et al. 2009; Taheri et al. 2009; Poursoltani and Gibling 2011; Robert et al. 2014).

Mozduran Formation (Oxfordian–Tithonian)

The Mozduran Formation is observed in W2 well and has a thickness of 270 m (see Figs. 4, 5; Table 2). This formation consists of dark gray micritic limestone, light gray crystalline dolomite, and dark gray oolitic limestone and has a conformable basal contact with the Kashafrud Formation. The Mozduran Formation comprises carbonates deposited during a marine transgression (post-rift subsidence of sedimentary basin) in Late Jurassic time (Golonka 2007; Kavoosi et al. 2009; Robert et al. 2014) (Fig. 4). Kavoosi (2014), on the basis of facies variation postulated this formation was developed in a deep-basin, fore-shoal, shelf margin, lagoon, tidal flat, and coastal plain depositional systems. This formation is the main gas reservoir in the KDM (Robert et al. 2014).

Zard/Shurijeh Formation (Berriasian–Hauterivian)

Kimmeridgian–Tithonian time is characterized by deposition of evaporites on the southern margin of the Scythian–Turan platform (Golonka 2007). In the eastern KDM, the Mozduran Formation is overlain by 100–1000 m of continental siliciclastics and evaporites of the Shurijeh Formation which was deposited during regression due to the late-Cimmerian tectonic phase (Seyed-Emami et al. 2004; Kavoosi et al. 2009) (Fig. 4). Hence, it seems that the eastern KDM was located in the southern margin of the Scythian–Turan platform in Tithonian time. Because of the peculiar arrangement of the lithologic units of the Shurijeh Formation (sandstone and siltstone capped by evaporites), this formation is

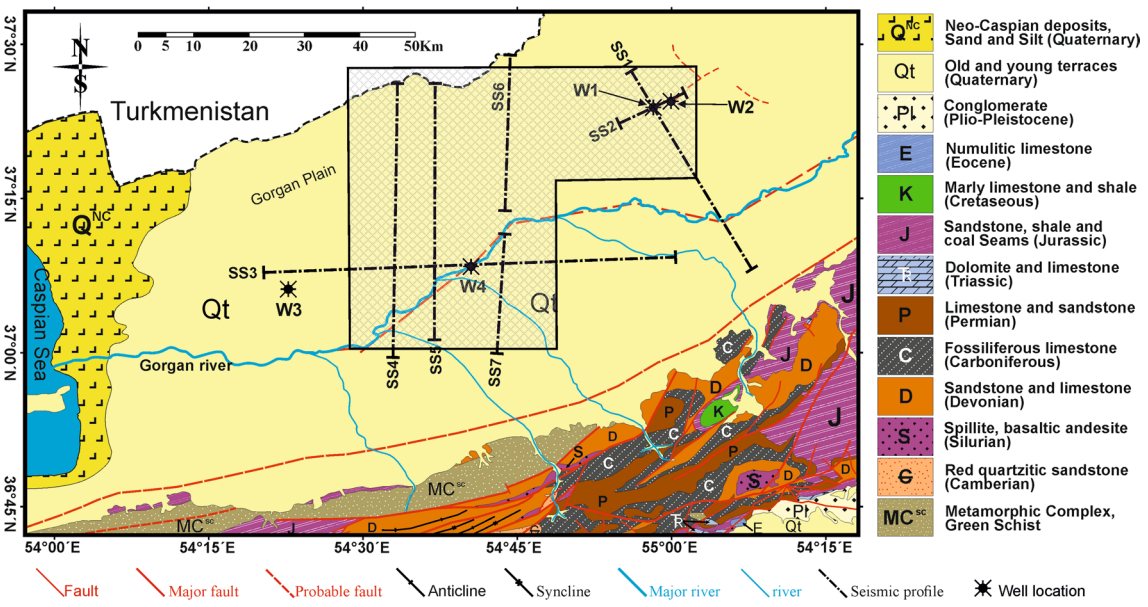

Fig. 3 Geologic map of the study area in the Gorgan Plain and the location of the acquired seismic profiles. The cross-hatched part shows the location of the TWT map of Fig. 13

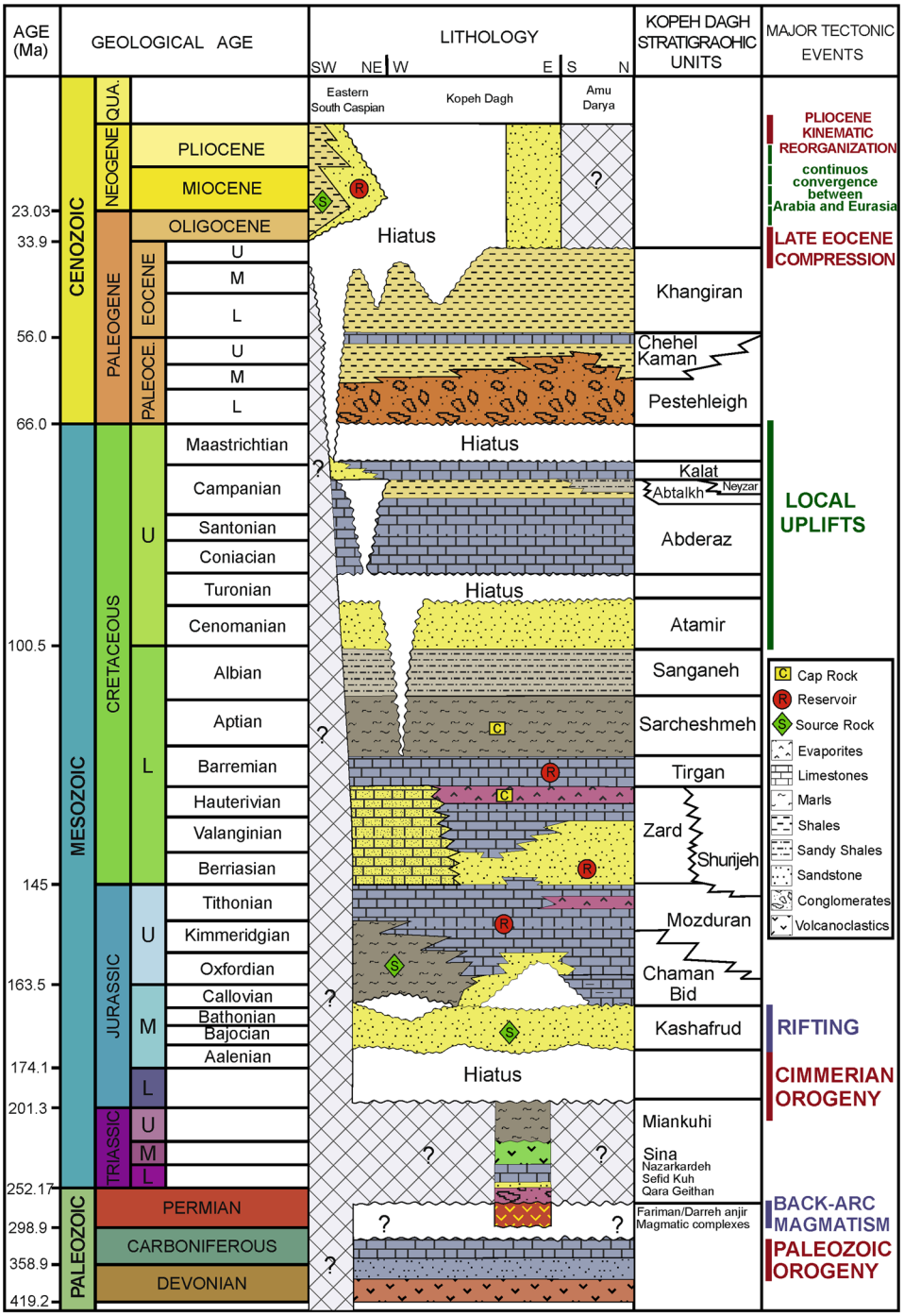

Fig. 4 Stratigraphic chart of the study area. Major tectonic events are shown on this stratigraphic chart and can be correlated with the main regional observed hiatus (Slightly modified after Robert et al. 2014). Tectonic event of the Permian period is adapted from Zanchetta et al. (2013)

a secondary gas reservoir of the KDM (Robert et al. 2014; Jozanikohan et al. 2015). Toward the west of KDM, the thickness of the Shurijeh Formation is decreased and laterally replaced by the Zard Formation, which mainly consists of marine marls and calcareous shale with some sandstone beds (Seyed-Emami 1975; Afshar-harb 1979; Robert et al. 2014; Kavoosi 2016). The Zard Formation thickness was measured to be about 1500 m in the W2 well (see Table 2; Fig. 5). This formation which was observed in W1 and W2 wells consists of an alternation of dark grey shale, marl, limestone, and siltstone.

Tirgan Formation (Barremian)

The Tirgan Formation consists of biointraclastic limestone (at the base), dark gray micritic limestone, and thin-bedded dark grey calcareous shale with a thickness of about 170–190 m in W1 and W2 wells (see Figs. 4, 5; Table 2).

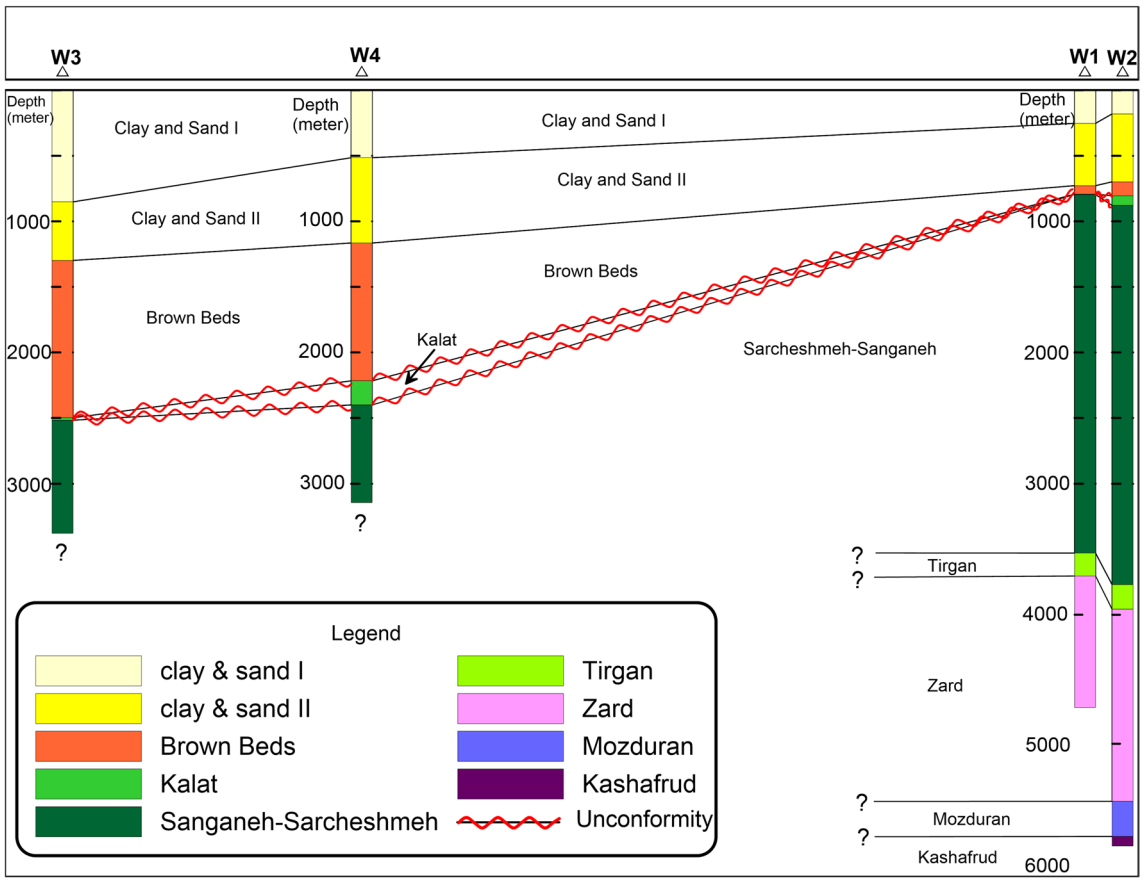

Fig. 5 Stratigraphic correlation among four wells in the study area. Modified from unpublished well reports of the Khazar Exploration and Production Company (KEPCO)

Because of post-rift subsidence of sedimentary basin concurrent with a global rise of the sea level, a transgression occurred during the Barremian time (Fig. 4). The marine sedimentation of the Tirgan Formation with thickness of 100–600 m conformably overlies the Shurijeh and the Zard formations in all of the KDM (Javanbakht et al. 2013; Robert et al. 2014). At the type section, Tirgan Formation mainly consists of bioclastic and oolitic limestone (at the bottom) and marls–shale (at the top) (Raisossadat and Moussavi-Harami 2000; Javanbakht et al. 2013; Robert et al. 2014).

Sarcheshmeh and Sanganeh formations (Late Barremian–Albian)

Due to the lack of any sharp boundary between the Sarcheshmeh and Sanganeh formations in diamond drilled wells in the Gorgan Plain (W1–W4), both of them are considered to be a single unit in this study (see Figs. 4, 5; Table 2). The thickness of this unit (the two Sarcheshmeh and Sanganeh Formations) measured about 2750 m in W1 well and about 2900 in W2 well. This unit shows monotonous lithologic characteristics and consists mostly of dark gray highly calcareous shale, marl and thin-bedded white chalky limestone. The contact between this unit with the Tirgan Formation is continuous in the W1 and W2 wells (Fig. 4).

The type section of Sarcheshmeh Formation includes two informal members, (1) the Lower marl (marls with thin-bedded limestone) and (2) the Upper shale (shale with limestone intercalations) (Raisossadat and Moussavi-Harami 2000; Robert et al. 2014). This formation shows various thicknesses ranging from less than 100 m in the eastern KDM to more than 1100 m in the western KDM (Aghanabati 2004).

In the type section, the Albian Sanganeh Formation consists of dark gray to black shale with greenish shale and local thin-bedded siltstone (Aghanabati 2004; Raisossadat 2006) (Fig. 4). Septarian nodules and cone-in-cone structures are abundant (Raisossadat 2006). The Sanganeh Formation varies in thickness from 750 m in the type section in the eastern KDM to more than 2000 m in the western KDM (Aghanabati 2004; Raisossadat 2006).

Kalat Formation (Late Maastrichtian)

The Kalat Formation is observed in all four wells logged in the Gorgan Plain and consists of limestone with intercalations of shale. Its thickness varies from about 4 m (in W1 well) to more than 180 m (in W4 well) (Table 2). In the type section, the Maastrichtian Kalat Formation consists mainly of detrital limestone with intercalations of shale and sandstone (Mahboubi et al. 2006; Hadavi and Notghimoghadam 2014) which conformably overlies the Sarcheshmeh and Sanganeh formations in the study area. However, its basal contact is an erosional surface (Figs. 4, 5; Table 2). Moreover, the top of the Kalat Formation was mostly eroded by an angular unconformity, but preserved from erosion inside the troughs. After deposition of the Sarcheshmeh and Sanganeh formations, a sedimentary hiatus happened in the western KDM (Berberian and King 1981) leading to a disconformity in Late Cretaceous (Afshar-Harb 1979).

Brown Beds (Pliocene)

The Brown Beds and younger formations are observed in all wells logged in the Gorgan Plain and vary in thickness from less than 100 m in the east to more than 1000 m in the west of the area (Table 2; Fig. 5). In the Gorgan Plain, the Pliocene Brown Beds (known as Red Bed Series or Productive Series in Turkmenistan and Azerbaijan, respectively) covers Cretaceous formations with an angular unconformity. This angular unconformity is clearly evidenced in all studied wells and seismic profiles of the Gorgan Plain (Table 2; Figs. 6, 7, 8, 9, 10, 11, 12). The Brown Beds Formation represents the most productive reservoir in the SCB, and is a thick prograding siliciclastic system deposited during a Lowstand System Tract (Smith-Rouch 2006). It is made up of light brown to yellowish brown sticky clay and greenish gray fine-grained sandstone. However, Buryakovsky et al. (2001) and Smith-Rouch (2006) reported some intercalations of siltstone and brown to dark gray shale within this formation.

Clay and Sand II (Late Pliocene–Early Pleistocene)

The Clay and Sand II with a more or less uniform thickness of about 500–600 m consists of blue gray to greenish gray sticky clay, gray and dark gray fine to medium-grained sandstone, gray unconsolidated sand and an unconsolidated oolitic beds (Fig. 5; Table 2). These sediments are equal to the Akchagylian and Apsheronian stages (Buryakovsky et al. 2001; Smith-rouch 2006; Torres 2007).

Clay and Sand I (Late Pleistocene–Holocene)

During Late Pleistocene–Holocene times, sedimentation continued under lacustrine environment, the Clay and Sand I sediments were deposited in the Gorgan region. The Clay and Sand I are made up of gray sticky clay, with abundant shell fragments and fine-grained unconsolidated sandstone.

Seismic data

Acquisition

To investigate the hydrocarbon occurrence in the regions around the southeast of Caspian Sea, an area with 3500 km^2 of 2D seismic profiles was obtained within the periods of 1960–1970 and 1992–1995 (Figs. 1, 3). The data were collected using dynamite (at depth of 4–30 m) as a source of seismic energy.

In this study, seven 2D seismic lines (SS1 and SS2 in Qezel-tapeh suite and SS3–SS7 in the Gorgan suite) were used to get a 2.5D model to enhance the structural view of the area. In fact, 2.5D model, known alternatively as pseudo-3D model, is a 3D simulation gained by 2D projection. In the Gorgan suite, the strike line (SS3) has an E–W direction with N–S X-lines (SS4, SS5, SS6, and SS7), and in the Qezel-tapeh suite strike-line (SS1) and X-line (SS2) have NNW–SSE and ENE–WSW directions, respectively. Acquisition geometry and parameters are listed in Table 1.

Processing

The seismic data were processed with advanced processing methods in noise reduction, velocity analysis, and migration algorithms. Continuous wavelet transform (CWT) methods were used for signal enhancement and dense velocity analysis was performed to obtain an accurate and correct velocity model to perform pre-stack time migration. Subsequently, correctness of time migration procedure was evaluated by migration evaluation techniques such as diffraction pattern reduction and preservation of continuity in seismic reflectors. Finally, migrated images were corrected by well data information.

Eleven wells have been previously drilled in the study area, of which four wells (W1, W2, W3 and W4) were used to gain data calibration. The seismic information from the studied wells are presented in Table 2 and correlations among these four wells are shown in Fig. 5. In this study, eight different horizons with different seismic properties have been identified from seismic data by utilization of version 2013 of Petrel computer software (Schlumberger). These horizons, from top to bottom, consist of Clay and

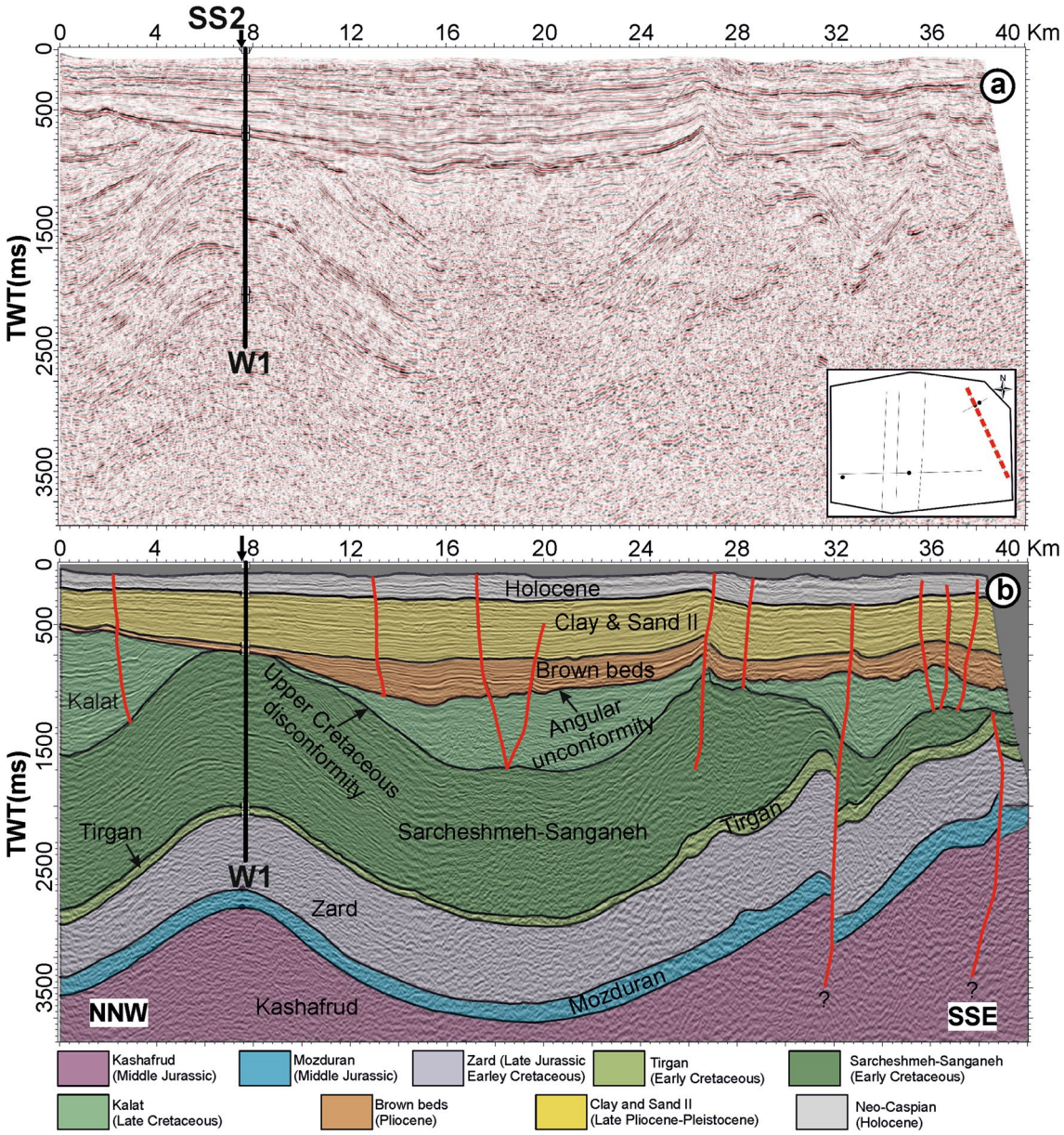

Fig. 6 **a** Uninterpreted time-migrated seismic profile SS1; the location of this seismic profile is marked by red dashed line in the base map (right side of the picture). **b** Structural interpretation of time-migrated seismic profile SS1. Two major reverse faults are shown in SSE part of the section, which are pre-normal faults (refer to "Discussion" section). Location of W1 well is marked in the seismic section. Downward black arrow indicates the location of the intersection with SS2 seismic profile

Sand II (Pliocene–Pleistocene), Brown Beds (Pliocene), angular unconformity (Paleogene), Upper Cretaceous disconformity, Tirgan Formation (Barremian stage), Zard/Shurijeh Formation (Lower Cretaceous series), Mozduran Formation (Upper Jurassic series) and Kashafrud Formation (Middle Jurassic series).

Tracing seismic reflectors or horizons was more difficult and less accurate in some areas due to locally poor quality of seismic data and lack of control points (particularly reasonable logs of the studied wells). In some seismic profiles (e.g., seismic section SS5), the seismic resolution is very low due to acquisition problems. In some profiles, quality was highly influenced by faults, which cause some uncertainties in interpretation of the seismic data.

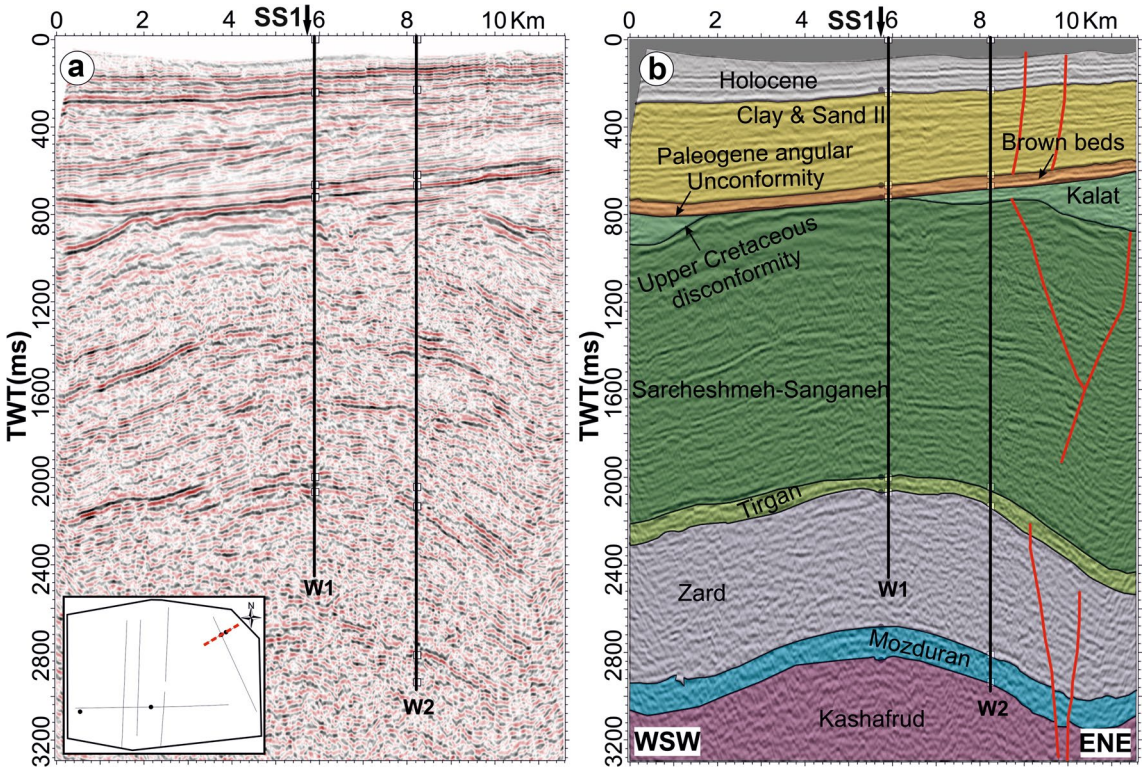

Fig. 7 **a** Uninterpreted time-migrated seismic profile SS2; the location of this seismic profile is marked by red dashed line in the base map (left side of the picture). **b** Structural interpretation of time-migrated seismic profile SS2. Angular unconformity is draped over a folded and partially exhumed Upper Cretaceous disconformity. A westward prograding system is identified in the Clay and Sand II Formation. W1 and W2 are diamond drill well locations. Downward black arrow indicates the location of intersection with SS1 seismic profile

Results

Seismic interpretation

Seismic Section 1 (SS1)

The 40 km-long seismic section SS1 in an NNW–SSE direction (Figs. 3, 6) revealed two unconformities. The lower unconformity occurs at the base of the Upper Cretaceous and appears as a disconformity. The upper unconformity is an angular one which was developed during the Paleogene by possibly the Late Eocene compressional tectonic phase. This orogeny brought about folding in the Jurassic and Lower Cretaceous formations and also folding of the Cretaceous disconformity in this area. An anticline and syncline beneath the Brown Beds and some reverse faults in the southeastern side of the profile are observed. These structural events gave rise to some drag folds in pre-Pliocene rocks. Some other fault-propagation folds in the post-Pliocene formations were interpreted in the seismic profile indicating that the area experienced a compressional tectonic regime. The angular unconformity merges with the Upper Cretaceous disconformity at the hinge of the anticline near the well W1 in Fig. 6 due to erosion of the Kalat Formation at the crest of the anticline. The profile also shows normal faults with minor offset in the post-Pliocene formations (Fig. 6).

Seismic section 2 (SS2)

The seismic section SS2 (Figs. 3, 7) is an 11.2 km-long seismic line trending in the ENE–WSW direction perpendicular to the SS1. This profile illustrates a gentle anticline in pre-Cretaceous sequences cut by a basal angular unconformity (Fig. 7). As in the SS1, the angular unconformity cuts down through the Upper Cretaceous disconformity at the hinge zone of the anticline. The Brown Beds dips down to the western side of the profile. A prograding sequence was discovered in the Pliocene sediments (Clay and Sand II) within this section indicating a drop in sea level during Pliocene. Four normal faults with little offset in pre-Cretaceous formations and two normal faults with little offset above the Brown Beds (Clay and Sand I and II) were recognized in this seismic section (Fig. 7).

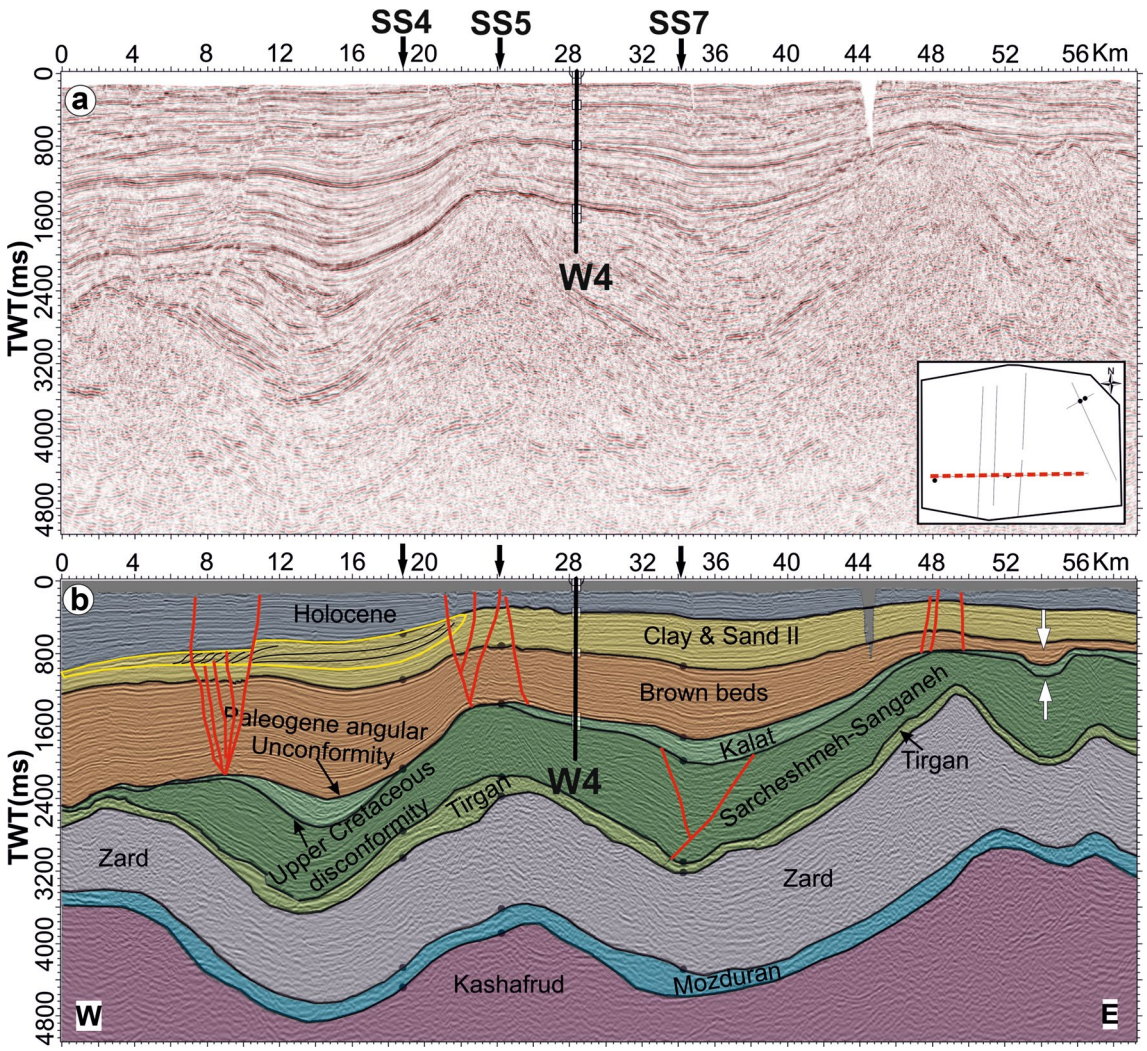

Fig. 8 **a** Uninterpreted time-migrated seismic profile SS3; the location of this seismic profile is marked by red dashed line in the base map (right side of the picture). **b** Structural interpretation of time-migrated seismic profile SS3. Note the normal faults located above fold hinges. White arrows denote the location of a huge channel which appeared in the closure of a syncline. Location of W3 well is given. Downward black arrows indicate the location of intersections with the SS4, SS5 and SS7 seismic profiles from west to east

Seismic section 3 (SS3)

This E–W trending section has 59.3 km long in the Gorgan Plain (Figs. 3, 8), and reveals that the post-Paleogene sediments are relatively thicker and dip westward in the study area. Almost sinusoidal folding occurred in the older formations, which are eroded and then cut by an angular unconformity. Also in this profile, the angular unconformity cuts through the Upper Cretaceous disconformity at the hinge zones of the anticlines. Some sets of normal faults appear in the Cenozoic formations above the hinge zones of the anticlines (Cretaceous basement may have a control on the location of faults) which may reflect the tensional stresses being produced over the hinge zones. A huge erosional channel is observed upon the angular unconformity (Fig. 8) which probably was a Paleo-river which was formed in the trough of the syncline. Finally, a prograding sequence is observed in the Pliocene Clay and Sand II sediments indicating the westward regression of the Caspian Sea during this period. The prograding sequence is intersected by a series of normal faults (Fig. 8).

Seismic section 4 (SS4)

The seismic section SS4 is a 50 km-long trending N–S across the Gorgan Plain toward the border of Turkmenistan (Figs. 3, 9). In this profile, the Lower Cretaceous and older formations are folded and reverse-faulted in the southern part of the section with little or no deformation in the northern part. Deformation in the southern part could

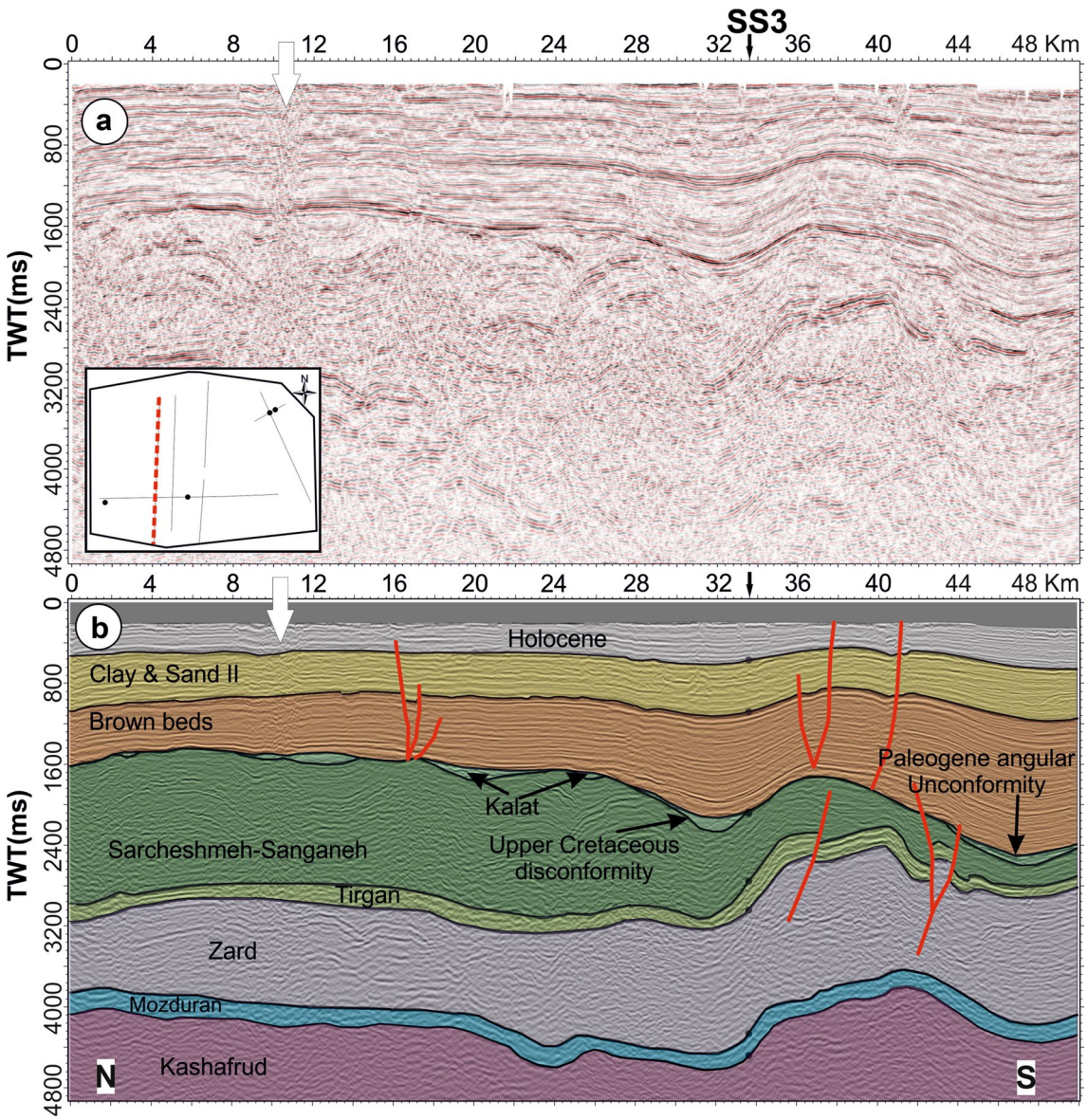

Fig. 9 **a** Uninterpreted time-migrated seismic profile SS4; the location of this seismic profile is marked by red dashed line in the base map (left side of the picture). **b** Structural interpretation of time-migrated seismic profile SS4. Note the pre-normal listric reverse faults in the Lower Cretaceous formations and normal faults of the post-Paleogene formations. White arrow denotes location of the probable gas chimney. Downward black arrow indicates the location of the intersection with the SS3 seismic profile

be related to the convergence of the Arabian block and Eurasia during Late Cretaceous–Early Paleocene period (Berberian and King 1981; Vernant et al. 2004; Hollingsworth et al. 2010). The angular unconformity mostly cuts the Cretaceous disconformity in this profile indicating the erosional processes during the phase of the Late Eocene compressional event were very strong. The Brown Beds Formation becomes thicker southward. A probable gas chimney is distinguished at the northern part of the profile marking the path of gas infiltration through the fractures of the post-Pliocene formations causing disturbance in the seismic reflectors (Fig. 9).

Seismic section 5 (SS5)

The 46 km-long seismic profile SS5 is 46 km, running parallel with the profile SS4 (see Figs. 3, 10). The Upper Cretaceous disconformity and the older formations were severely folded and cut by a major reverse fault in the northern part of the profile. The Pliocene series have experienced gentle folding and normal faulting at anticline hinges. Like the SS4 seismic section, this profile also shows southward thickening of the Brown Beds Formation. The angular unconformity also cuts through the Upper Cretaceous disconformity, especially where the Brown Beds thicken southward.

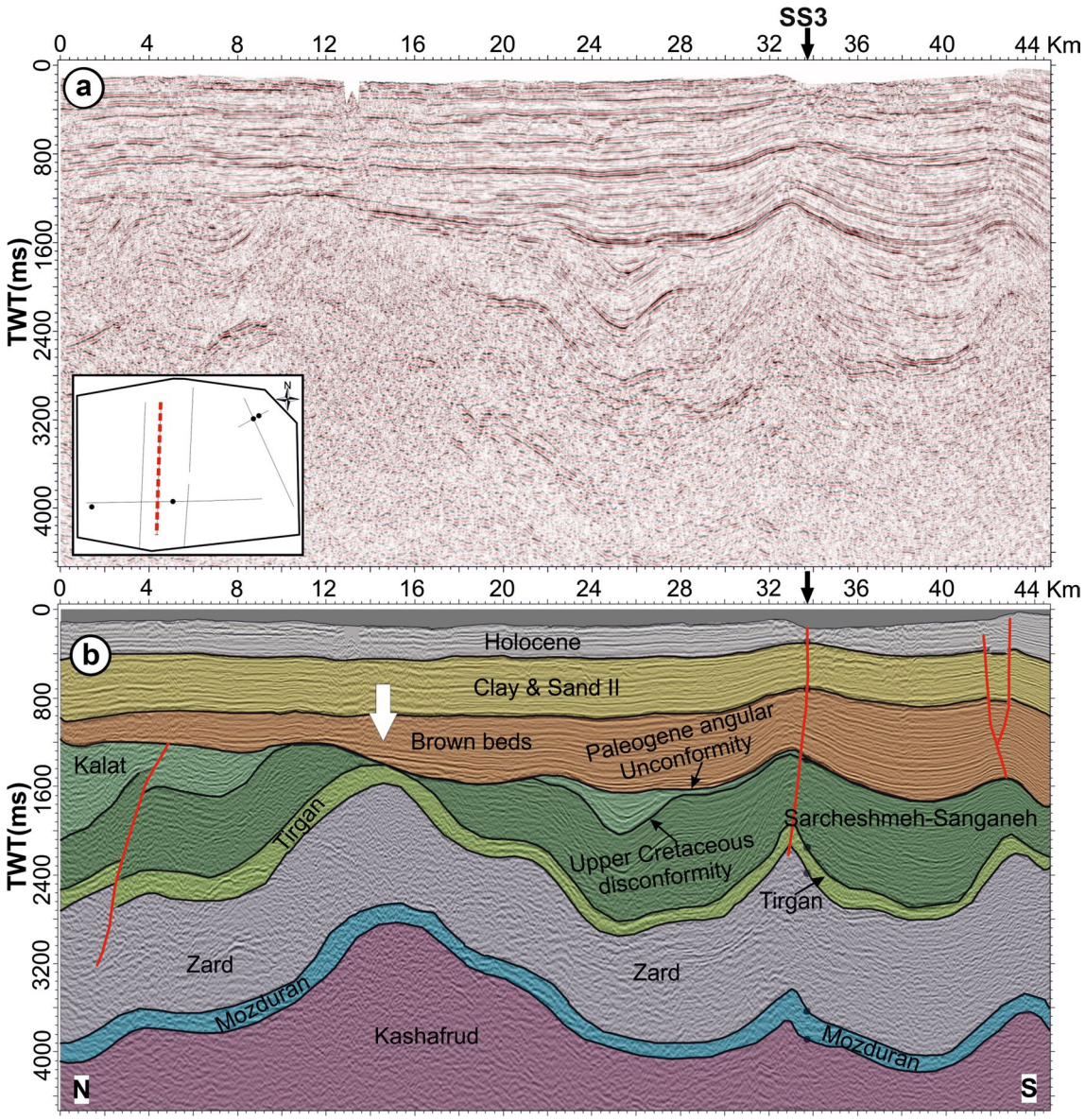

Fig. 10 **a** Uninterpreted time-migrated seismic profile SS5; the location of this seismic profile is marked by red dashed line in the base map (left side of the picture). **b** Structural interpretation of time-migrated seismic profile SS5. An anticline appears in the center of the seismic profile (specified by the white arrow) seemingly belongs to a local pop-up structure formed due to an NNE–SSW strike-slip system. The resolution of the profile is very low at this part so faults are indistinguishable, but the body of pop-up structure was identified. Continuation of this local pop-up is visible in the SS6 seismic profile in Fig. 11. Downward black arrow indicates the location of intersection with the SS3 seismic profile

Seismic section 6 (SS6)

The seismic section SS6 is 28 km running N–S direction and reaches to the border of Turkmenistan (see Figs. 3, 11). The Upper Cretaceous disconformity was eroded away—leaving an angular unconformity at the hinge zones of the anticlines. In the northern end of the section, a transpressive strike-slip fault system formed a local pop-up structure beneath the Brown Beds. The Brown Beds Formation thickens toward the south of the profile. No deformation is evident in the Pliocene and younger formations suggesting that the northern area did not experience any tectonic compression after the angular unconformity.

Seismic section 7 (SS7)

This section is 21.5 km and runs parallel and to the seismic profile SS6 (Figs. 3, 12). The angular unconformity cuts the Upper Cretaceous disconformity in both ends of the profile. In the central part of the profile, shale from the Zard

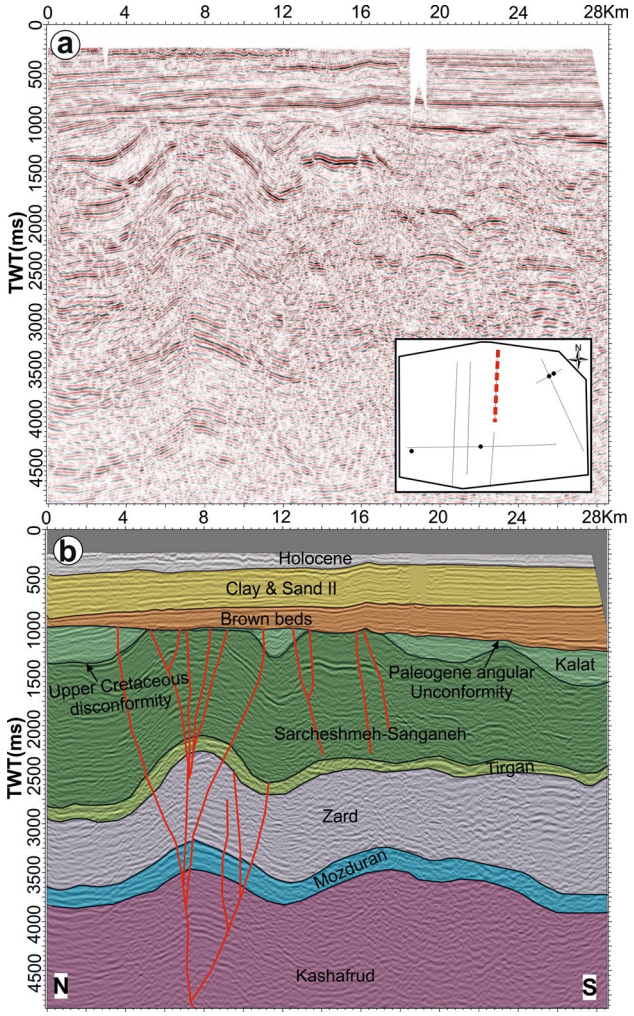

Fig. 11 **a** Uninterpreted time-migrated seismic profile SS6; the location of this seismic profile is marked by red dashed line in the base map (right side of the picture). **b** Structural interpretation of time-migrated seismic profile SS6. A pre-Paleogene strike-slip system is clearly visible in this seismic profile which caused a local pop-up structure and became eroded in the subsequent orogenic phases

Formation penetrates through (in a diaper-shape pattern) the Tirgan Formation, Sarcheshmeh–Sanganeh and Kalat formations. The Brown Beds, Clay and Sand II and Holocene rocks have an antiformal structure over the Zard diapir and are also faulted.

Horizon modeling

Eight different stratigraphic boundaries have been identified in studied seismic sections and converted into two-way-time (TWT) maps along with these stratigraphic units. All of the eight TWT maps were generated with an increment of 50 m (see Fig. 13).

The TWT maps for the tops of the lowermost Kashafrud and Mozduran formations are very similar (Fig. 13a, b), because the Mozduran Formation shows minor variations in thickness in the studied seismic sections (see Figs. 5, 6, 7, 8, 9, 10, 11, 12). In fact, the top of the Mozduran Formation mimics the top of the Kashafrud Formation. Both formations are in relatively shallower depths toward southeast and get deeper westwards and northwestwards. There is evidence for NE–SW folding in northeast of the area, and also for weak dome and basin interference pattern in the central parts of the area. Deep reverse listric faults in the southeast of the area run SW–NE broadly parallel to the folding in the northeast of the area. The pronounced dome structure in the center of the map is associated with NNE trending strike-slip faults giving rise to an antiformal pop-up structure in the central part of the area (Fig. 13a, b).

The tops of the Zard and Tirgan formations also have similar geometric characteristics due to almost uniform thickness of the relatively thin Tirgan Formation, except where the Zard Formation diapirically penetrated through the Tirgan Formation (Fig. 13c, d). The Tirgan limestone gives a strong seismic impedance (limestone against shales and marls) making it easy to trace the Tirgan Formation. The Tirgan and Zard formations lie at relatively shallower depth in the SE and dip down to the northwestern part of the study area. The SW–NE trending fold is still present in the NE, but the central area is dominated by well-developed dome and basin pattern. This relates, in part, to the diapiric rise of the Zard Formation along the seismic profile SS7 (SE of W4 well). Deep reverse listric faults, appearing in the south of the area, are parallel to the trends of the Eastern Alborz mountain chain and western termination of the KDM. A major dome structure in the north of the area seems to be associated with NEN trending strike-slip faults; but due to the locally low resolution of the seismic profile in this part, the faults can hardly be traced Fig. 10.

The Upper Cretaceous disconformity is difficult to map because in places there seems to be continuous sedimentation without significant erosion. In this case, the obtained data demonstrate the erosional nature of this marker supported by paleontological studies on cores and cuttings in wells W2, W3 and W4 (Fig. 5). The disconformity lies at shallow depth in the east and dips generally to the west (Fig. 13e). The deep reverse listric faults are absent, but the NE–SW strike-slip fault system persists in the central region, though the pronounced dome which is in relation to strike-slip fault system disappears. There are NE–SW trending folds in the east and well-developed dome and basin structure in the central part of the region. The Cretaceous disconformity was eroded by angular unconformity at the hinge of anticlines and was wholly eliminated at the western part of study area.

Due to the unique and specific seismic characteristics, some horizons such as Brown Beds and angular unconformity can be readily recognized. The angular unconformity,

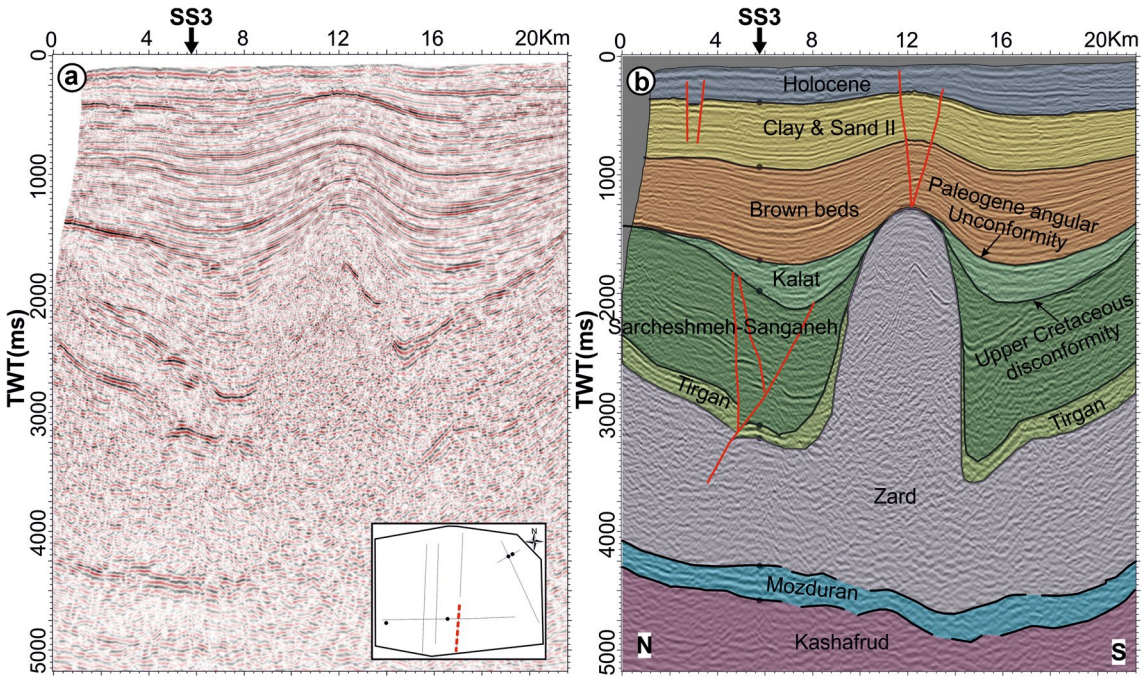

Fig. 12 **a** Uninterpreted time-migrated seismic profile SS7; the location of this seismic profile is marked by red dashed line in the base map (right side of the picture). **b** Structural interpretation of time-migrated seismic profile SS6. The Zard unit has formed a diapiric structure penetrating upward into the Tirgan, Sarcheshmeh and Sanganeh, Kalat formations. Downward black arrow indicates the location of intersection with the SS3 seismic profile

Table 1 Geometry of the seismic line used in this study

Mid-point and offset geometry		Shot and receiver geometry	
CMP numbers	1900	Number of shots	680
Maximum fold	35	Shot spacing	70 m
CMP spacing	25 m	Number of receiver	99
		Receiver spacing	50 m
Frequency content		Recording parameters	
Frequency range	8–100 Hz	Total recording time	7 s
Dominant frequency	20 Hz	Sampling interval	4 ms

because of angular differences and existence of top-lapped seismic reflectors, is the most reliable seismic marker in the area (Fig. 6, 7, 8, 9, 10, 11, 12, 13f). This unconformity appears at shallow depths (< 1000 m) in the east and reaches to depths > 2000 m in the west (Fig. 13f). Some NE–SW normal faults appear in the east of the area. Folds with The NE–SW trending folds becomes disappeared, and only a weak dome and basin interference pattern is visible in the south and central parts of the area.

The tops of the Brown Beds and the Clay and Sand II formations have similar geometrical properties (Fig. 13g, h). Both formations dip westward and lie near the surface in northeast of the area. The thickness of Brown Beds varies from a few meters to over a 1000 m in eastern and western parts of the study area, respectively. The Clay and Sand II Formation, however, shows more or less uniform thickness through the entire area (Figs. 6, 7, 8, 9, 10, 11, 12), explaining why the tops of both formations have similar patterns in Fig. 13g, h. Two sets of normal faults trending N–S and NE–SW are seen to cut the tops of both formations. Also, a gentle dome and basin interference pattern is visible.

Structural setting

In this section, we will discuss results from the seismic sections and the wells, and introduce the structural setting on

Table 2 Information on four studied wells drilled in the study area

Time units	Numerical age (Ma)	Rock units	W1	W2	W3	W4
Quaternary						
Holocene	Present	Clay and Sand I	0	0	0	0
Pleistocene	0.0117	Clay and Sand II	252.07	180.14	851.26	514.35
Tertiary						
Neogene						
Pliocene	2.58	Brown Beds	727.56	698.3	**1298.13**	**1165.1**
Miocene	5.333	Hiatus	Angular unconformity at the depth of 792.17 m	Angular unconformity at the depth of 804.98 m	Angular unconformity at the depth of 2498.73 m	Angular unconformity at the depth of 2216.66 m
Paleogene						
Oligocene	23.03					
Eocene	33.9					
Paleocene	56.0					
Cretaceous						
Late	66.0	Kalat	792.17	804.98	2498.73	2216.66
		Hiatus	Erosional surface at the depth of 795.83 m	Erosional surface at the depth of 878.59 m	Erosional surface at the depth of 2517.35 m	Erosional surface at the depth of 2400.76 m
Early	100.5	Sarcheshmeh-Sanganeh	**795.83**	878.59	2517.35	2400.76
		Tirgan	**3528.67**	**3769.16**	–	–
		Zard/Shurijeh	3703.62	**3956.61**	–	–
Jurassic						
Late	~145.0	Mozduran	–	**5422.7**	–	–
Middle	163.5 ± 1.0	Kashafrud	–	5690.92	–	–
Early	174.1 ± 1.0	Not reached	–	–	–	–
Triassic						
Late	201.3 ± 0.2	Not reached	–	–	–	–
Well total depth below the rotary table			4706.42	5763.46	3377.49	3143.4
Rotary table elevation referred to Caspian Sea level			+52.73	+59.44	+18	+35.81

Well depths (in m) are to the top of individual formations. Bold cells characterize the formations with hydrocarbon occurrences (commercial and non-commercial). Numerical ages of time units were adapted from Cohen et al. (2013)

the basis of interpretations of the seismic profiles. The main aim is to provide an optimal model for structures in the studied area and their potential for developing hydrocarbon traps.

Structures of the Gorgan Plain are divided into two main groups. The first group predates the angular unconformity and the second postdates it. Below the angular unconformity, the Mesozoic faults are subdivided into two series, (1) deep reverse listric (Figs. 6, 9) and (2) strike-slip (Fig. 11). Deep reverse-listric faults are located in the south of the studied area, and have an overall strike of ENE–WSW and northward dip (Figs. 6, 13a–d). These faults are parallel to the Eastern Alborz and the western termination of the KDM. Based on the listric geometry, it is likely that these deep listric faults were originally normal faults formed under the tensional regime after the Eo-cimmerian orogeny (post-orogenic rifting). Later, due to the closure of Neotethys Ocean, the Eo-cimmerian normal deep listric faults inverted and acted as reverse faults during the Late Eocene compressional tectonic event. A second series of Mesozoic faults are mainly of strike-slip type in the north and center of the studied area. They are associated with a local antiformal pop-up structure in the Mesozoic sedimentary erathem (Figs. 11, 13a–d). The strike-slip faults have a NE–SW trend and terminate at the top by an angular unconformity (Fig. 11) indicating a pre-Paleogene age. Based on the lack of activity in the Cenozoic sequences, and the orientation of these fault systems with respect to the Paleotethys suture zone, it seems likely that these strike-slip faults formed under a transpressional condition during the Late Eocene tectonic event. Some other south-dipping reverse faults in the south of this strike-slip faults are terminated by the angular unconformity (Fig. 11).

As with the faults, folding of the Mesozoic sedimentary erathem in the area shows two sets of structures. In the east and northeast of the studied area, there are folds whose axial planes have overall ENE–WSW trend (parallel to the Eastern Alborz, the western KDM, and the deep reverse listric faults). In the center and south of the studied area, there is a dome and basin interference pattern (Fig. 13a–e).

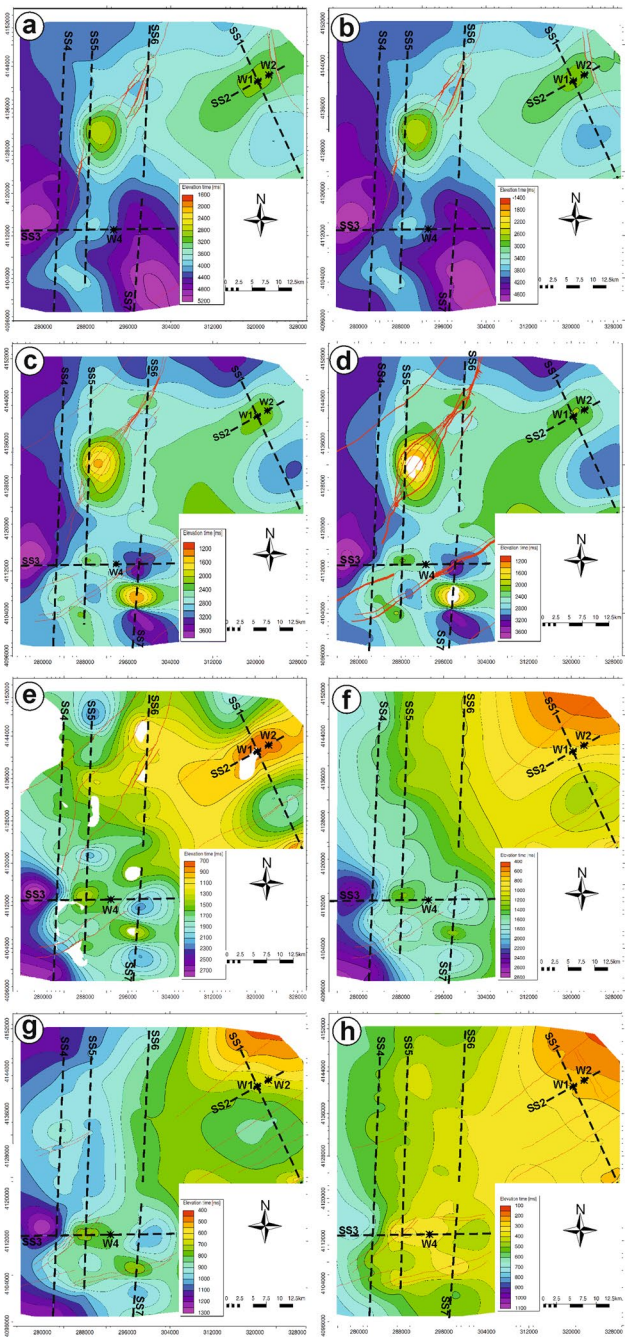

Fig. 13 Structural TWT map of eight top formations of the studied area. **a** Kashafrud Fm. and **b** Mozduran Fm., both formations appear in shallow depths in the east of the area and dips westerly. **c** Zard Fm. and **d** Tirgan Fm., The NE–SW trending structures are weakened and dome–basin interference pattern is clearly observable in these two formations. **e** Cretaceous disconformity was eroded in the west of the area by angular unconformity. Dome-basin interference pattern is still sensible. **f** Angular unconformity. This unconformity is eroded the Cretaceous disconformity in the crest of anticlines. The NE–SW normal faults are related to the tension above the hinge of underneath anticlines. **g** Brown Beds. Likewise the angular unconformity, this top formation shows normal faults above the hinge zone of anticlines. Dome-basin interference pattern can be seen in this top formation but the predominance of NE–SW folding is ended. **h** Clay and Sand II. This top formation shows minimum deformation and the NE–SW folding. It seems that the NNW–SSE trend is the dominant deformation. The location of the seismic profiles and wells are also marked

Since the Mozduran and Tirgan formations contain rock units with reservoir characteristics, the folding of the Mesozoic sedimentary erathem was also capable of producing structural traps for accumulation of hydrocarbon materials in the hinge zone of the anticlines (see Fig. 4). The parallel orientation of the ENE–WSW trending Mesozoic erathem folds, along with deep reverse-listric faults and their truncation by the angular unconformity at the base of the Cenozoic erathem, indicates their simultaneous formation in the Late Eocene compressional event.

The Upper Cretaceous disconformity is folded by the Late Eocene compressional event and predominantly preserved in the syncline cores as shown in wells W2, W3, and W4. Based on the timing (post-Albian–Aptian Sarcheshmeh/Sanganeh formations and pre-Maastrichtian Kalat Formation) and characteristics of this erosional surface, we suggest that it relates to the Late Cretaceous event (Aghanabati 2004) that caused the local uplift and creation of the Cretaceous disconformity in the Gorgan Plain before the Late Eocene compressional deformation and further uplift (Fig. 4). After a period of erosion, the Pliocene Brown Beds were deposited with angular unconformity on the folded Cretaceous disconformity and sedimentary systems (best seen in Figs. 6, 7, 10, 11). The angular unconformity merges gradually to the west with the top Cretaceous disconformity and at the hinge zone of the anticlines where the Cretaceous disconformity was folded (Fig. 6, 7, 8, 9, 10, 11, 12).

Based on sedimentary hiatus during the Paleogene time and the angular relationship between the Upper Cretaceous and Pliocene sedimentary series, it seems that the aforesaid angular unconformity was formed during the Late Eocene compressional event (Figs. 4, 5). In fact, three structural events occurred concurrently in conjunction with the appearance of the angular unconformity, (1) mechanism inversion of deep listric reverse faults, (2) creation of the strike-slip system, and (3) folding of the Mesozoic erathem (including the Cretaceous disconformity).

Above the angular unconformity, Cenozoic faults are divided into two sets, (1) normal and (2) strike-slip with two different trends of N–S and NE–SW, respectively (Figs. 8, 13h). The normal faults occur above the anticlinal hinge zones of the folded Mesozoic erathem. For the Cenozoic sedimentary erathem, ENE–WSW folding is not visible and, instead, a weak dome and basin interference pattern is observable (Fig. 13h).

Discussion

Based on the given results obtained by seismic analyses, interpretations and gridding of eight horizons in the Gorgan Plain, it was deduced that Gorgan Plain and adjacent regions are highly influenced by structural inheritance and

several extensional and compressional events related to the closure of the Paleotethys (Cimmerian orogeny) and later by the closure of Neotethys Ocean. Structures of the study area could be divided into two main groups. The first group with a compressional regime predates to angular unconformity, and includes reverse faults, thrusts, and folds that occur parallel to the Alborz and western terminations of the KDM belts having overall NE–SW trends. Reverse faults were former normal faults which formed during the post-Cimmerian orogeny rifting and later inverted and acted as reverse faults during the Late Eocene compressional phase (Stöcklin 1968, 1974; Brunet et al. 2003; Allen and Armstrong 2008; Allen et al. 2011; Rezaeian et al. 2012). Folding of the pre-Paleocene formations occurred simultaneously with inversion of the normal faults (Late Eocene compressional tectonic phase). The second group of structures includes normal faults which occurred in post-Pliocene formations. Actually, the left lateral movement of the Alborz in the south and the right lateral action of the Ashgabat fault in the north of the study area caused westward extrusion of the SCB (e.g., Jackson et al. 2002; Allen et al. 2003a, 2006; Hollingsworth et al. 2006; Robert et al. 2014). Due to this westward extrusion, some strike-slip systems formed causing the development of a few basins and pop-up structures in the Gorgan Plain for the post-Pliocene formations. Furthermore, westward extrusion of the SCB brought about superimposition of a new series of folds on pre-Paleocene structures. These refolded structures formed the dome and basin interference pattern, wherein each dome is surrounded by four basins and each basin is surrounded by four domes (Ramsay 1962; Grasemann et al. 2004).

An explanation to this refolding event might lie in the reorganization of the Arabia–Eurasia collision zone at ~5 Ma. Allen et al. (2003b) declared that compressional deformation of the Alborz began in the Miocene due to early stages of Arabia–Eurasia collision. They introduced conjugate right-lateral and left-lateral faults in the west and east of the Alborz, respectively (Allen et al. 2003b). On the other hand, they noted that there was a little or no lateral movement of SCB relative to Iran (Allen et al. 2003b). Therefore, it is reasonable to say that the first stage of folding in the Gorgan Plane happened under compressional condition. Afterward, reorganization of Arabia–Eurasia collision (~5 ma) caused westward migration of SCB, reversal in slip sense of Western Alborz and left-lateral movement of Eastern Alborz (Allen et al. 2003b). Simultaneous left-lateral and right-lateral movement of Eastern Alborz (to the south of Gorgan Plain) and Ashgabat fault (to the north of Gorgan Plain) (Jackson et al. 2002; Allen et al. 2003a, b, 2006; Hollingsworth et al. 2006; Robert et al. 2014) probably caused a local change in the stress direction inside the Gorgan Plain. This local change in the stress direction from N–S to E–W caused second series of folds with N trending, which overprinted upon the first series of folds with ENE trending (Fig. 14). Furthermore, Torres (2007) introduced five sub-parallel fold trends in the Pliocene strata of Western Turkmenistan. These folds are parallel to the South Caspian Sea shoreline (Torres 2007). Therefore, it seems that these folds formed as a result of westward movement of SCB. In other words, since Pliocene times, Western Turkmenistan and perhaps Gorgan Plain deformed due to the SCB resistance against inward compression from the east (second stage of folding).

Deep reverse listric faults with an ENE–WSW trend in the south of the study area formed during post-Cimmerian tensional regime as the normal faults were later inverted into reverse faults during the Late Eocene compressional event. Due to the rifting (post-Cimmerian orogeny), deposition of the Shemshak Group and the Kashafrud Formation took place in the Alborz and KDM, respectively (these successions probably were deposited in the same regional basin) (Fürsich et al. 2009b; Taheri et al. 2009; Kavoosi et al. 2009; Poursoltani and Gibling 2011). Considering the low porosity and low permeability levels of the sandstones, the Kashafrud Formation is inferred to be a potential reservoir for hydrocarbon (Poursoltani and Gibling 2011).

Then, sedimentation continued in the region by deposition of the marine sediments of Mozduran, Zard, Tirgan, Sarcheshmeh, and Sanganeh Formations. From a petroleum point of view, the carbonates of the Mozduran and Tirgan formations are the reservoirs of the region (Javanbakht et al. 2013; Robert et al. 2014; Kavoosi 2016). Based on the dome and basin interference pattern observed in the Gorgan Plain, and the function of Sarcheshmeh Formation as a cap rock, the two formations can potentially form anticlinal traps for the hydrocarbon materials. The ongoing sedimentation of the KDM continued until the Upper Cretaceous, when the localized uplift caused a hiatus and the Upper Cretaceous disconformity formed (Afshar-Harb 1979; Berberian and King 1981). Furthermore, Berra et al. (2007) introduced a major angular unconformity at the base of the Upper Cretaceous successions in the Neka valley (northern flank of the Alborz in vicinity of the Gorgan Plain), indicating the presence of emerged land which persisted during Jurassic and most of the Cretaceous period. Robert et al. (2014) suggested that several local tectonic uplifts occurred in the southern part of the Amu Darya Basin during the Late Cretaceous without angular unconformity. The Upper Cretaceous disconformity which is recorded in the study area corresponds to these local tectonic emerged lands. Following this erosional surface, the upper Maastrichtian Kalat detrital sediments were deposited in the study area (Berberian and King 1981) which were mostly eroded by an angular unconformity, but preserved from erosion inside the troughs. The lack of Paleogene sediments of the KDM in the Gorgan Plain

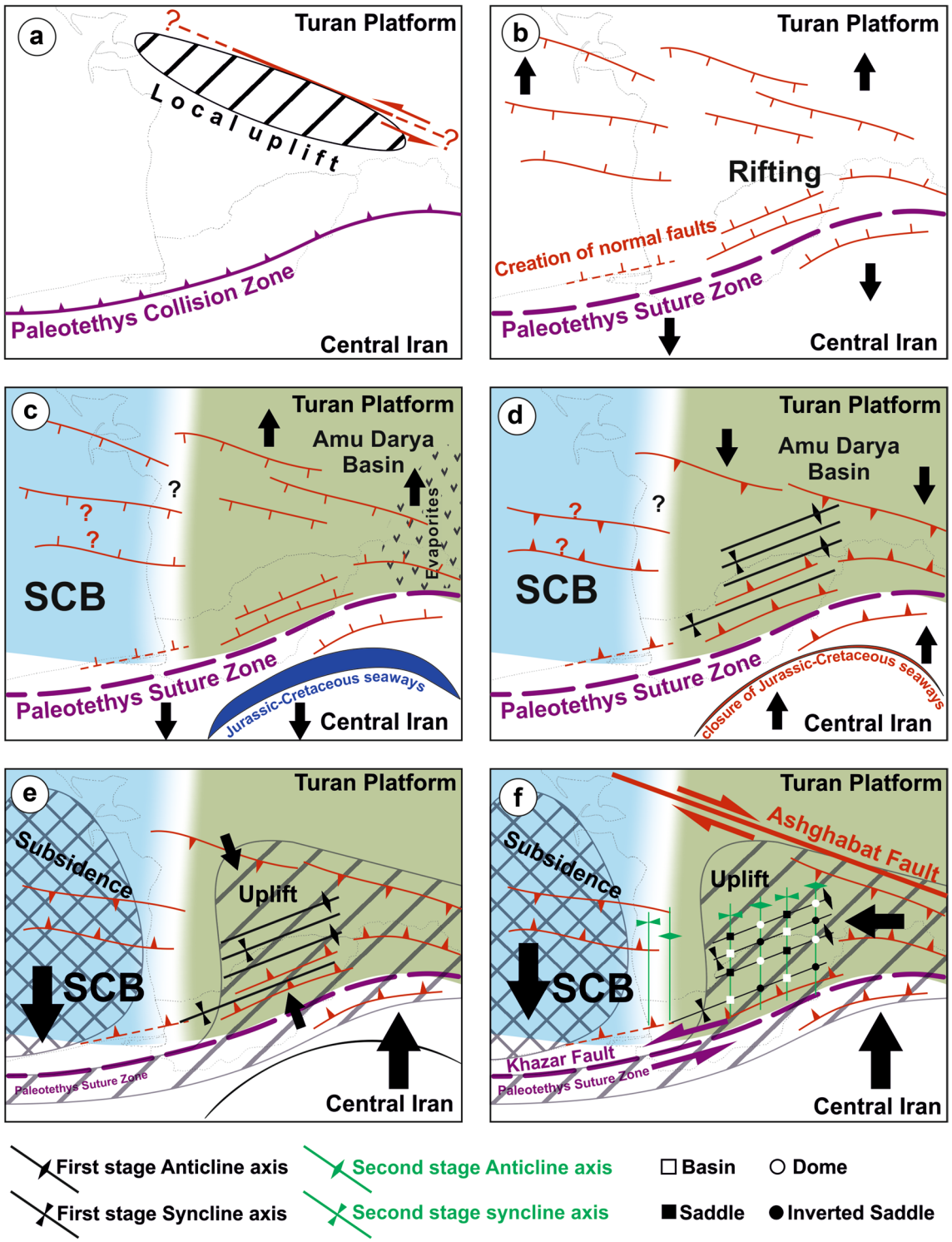

Fig. 14 Schematic reconstruction of the structural evolution of the Gorgan Plain during **a** Late Triassic–Early Jurassic; **b** Middle Jurassic; **c** Late Jurassic–Early Cretaceous; **d** Late Cretaceous–Paleocene; **e** Late Eocene–Oligocene; and **f** Pliocene–Pleistocene until recent. Reconstructions of the Paleotethys suture zone and the Jurassic–Cretaceous narrow seaways were adapted from Robert et al. (2014)

(Paleogene successions are absent in diamond drill wells in the Gorgan Plain) is an indication that erosion was activated for the Gorgan Plain during this period. In fact, this area emerged during the Late Eocene compressional event, and uplifting and deformation occurred concurrently. As a result, during Paleogene, erosion occurred

instead of sedimentation in the Gorgan Plain. Variation in mechanism of the faults (from normal to reverse) occurred during this period. Aghanabati (2004) indicated that the Late Eocene compressional event caused inversion of pre-normal faults into thrust and reverse faults in northern Iran. This orogeny also resulted in the formation of right lateral strike slip faults trending NW–SE, and left lateral faults trending NE–SW. Reverse faults, observable in the south of the area, indicate that the concomitant compression from the Alborz was active in the area and caused fault-related folding in the Brown Beds and younger formations. In other words, it seems that folding of the angular unconformity in the south of the study area is due to induced compression from the Alborz (simultaneously accompanied by erosion) during the Paleocene–Early Pliocene period. The emergence of the study area under the forces of the Late Eocene compressional event continued till late Oligocene–Early Miocene, and then a transgression happened and the Maykop suite was deposited in the SCB (Smith-rouch 2006; Torres 2007). The Maykop suite, which is the principal hydrocarbon source rocks in the SCB, is not observed in the studied wells, and this is a proof of the simultaneous emergence of the area and intensive erosion during the Oligocene–Early Pliocene.

Following the angular unconformity, clastic sediments of the Brown Beds and Clay and Sand II represent a continental environment for the deposition of these formations. Substantial thickness variation in the Upper Pliocene–Lower Pleistocene formations toward the west of the study area and appearance of the dome and basin interference pattern in these formations provide sufficient evidence for simultaneous sedimentation and tectonic activity in the region. Furthermore, the prograding sequences observed in the Clay and Sand II Formation demonstrate the westward regression of the Caspian Sea and tectonic activity. This westward regression is probably as a result of simultaneous uplifting of the KDM and westward extrusion of the SCB relative to Eurasia and Central Iran. The westward movement of the SCB happened as a result of left-lateral action of Khazar fault in the south and right-lateral movement of the Ashgabat fault in the north of the Gorgan Plain (e.g., Lyberis et al. 1998; Jackson et al. 2002; Allen et al. 2006; Ritz et al. 2006; Hollingsworth et al. 2008; Bretis et al. 2012). The onset of westward extrusion of the SCB is contentious. Based on speed of motion of the SCB, Alborz, and KDM, Jackson et al. (2002) stated that this westward extrusion commenced in Pliocene, whereas Hollingsworth et al. (2006, 2008) argued that this westward movement began ~ 10 Ma (since Miocene). However, Ritz et al. (2006), based on morphotectonic evidence and structural analysis, suggested that the movement started since Pleistocene. In this paper, on the basis of simultaneous tectonic activation and sedimentation during the Pliocene–Pleistocene and appearance of the dome and basin interference pattern in the Pliocene and younger formations, we believe that the onset of westward extrusion of the SCB was late Pliocene–early Pleistocene.

Due to the westward extrusion of the SCB, earlier folds (which formed during the Late Eocene compressional deformation phase) were refolded into a dome and basin interference pattern. During this refolding phase, some strike-slip faults formed which affected post-Paleogene formations and some pop-up structures were also developed. In general, the development of an angular unconformity, a disconformity, superimposed folds, and inversion of normal faults show a complex pattern of tectonics since the Jurassic. This pattern of tectonics (especially, dome and basin pattern) led to the development of the potential hydrocarbon traps in the Gorgan region.

Conclusion

The structural and geophysical survey of the studied area demonstrated that the Gorgan Plain in the southeastern boundary of the South Caspian hydrocarbon basin is characterized by several regressive–transgressive sequences and some epeirogenic and orogenic phases since the Lower Jurassic. Tectonic history and evolution of the region are a result of convergence of the Gondwanan-derived terranes and Eurasia.

The most important result of this work is the identification of dome and basin interference patterns of folding, which formed due to a local change in the direction of predominant tectonic compression. This direction change caused superimposition of a new E–W trending folds upon the previous NE–SW trending ones. Based on the lithological characteristics and arrangement of the formations (see Fig. 14), the resultant dome and basin could have produced structural traps in the crest of the domes.

The angular unconformity can be regarded as the boundary between changes in the direction of the predominant compression regime inside the area (from N–S to E–W). In other words, we suggest that the local change in direction happened during the Pliocene–Pleistocene period. In fact, the collision between the Arabian Plate and the southern margin of Central Iran happened in the Late Eocene–Oligocene. Since Late Eocene–Pliocene, substantial deformation took place throughout the Iranian Plateau such as lengthening along the Arabia–Eurasia suture zone. During Early Pliocene, the Afghan–India collision sealed the eastern free-face of the suture zone. This event resulted in kinematic reorganization of the Arabia–Eurasia convergence and acceleration of shortening and exhumation around the Central Iranian micro-continent. The kinematic reorganization of the Arabia–Eurasia convergence caused the Khazar fault to act as a left-lateral fault to the south and the Ashgabat

fault to act as a right-lateral fault to the north of the Gorgan Plain. The conjugate action of these two faults caused a local direction change in predominant tectonic compression and resultant dome and basin interference pattern.

Acknowledgements This research was derived from the Ph.D thesis of the first author and supported by the Khazar Exploration and Production Company (KEPCO). Our special thanks go to the authorities of KEPCO, especially the exploration directorate, for their generous collaboration and furnishing of technical support. The authors also are very grateful to Prof. Ali Asghar Calagari and Dr. Alan Boyle for critical reading of the early draft of our manuscript. The critical and thoughtful reviews of the manuscript by Dr. Andrea Zanchi and Prof. Mark Allen are highly appreciated. Our thanks are further extended to Prof. Wolf-Christian Dullo for editorial handling of the manuscript.

References

Abrams MA, Narimanov AA (1997) Geochemical evaluation of hydrocarbons and their potential sources in the western South Caspian depression. Repub Azerb Mar Pet Geol 14:451–468

Afshar-Harb A (1979) The stratigraphy, tectonics and petroleum geology of the KopetDagh region, northern Iran (Ph.D. Thesis). Imperial College London (University of London)

Aghanabati A (2004) Iran geology. Publication of Geology Organization **(in Persian)**

Alavi M (1996) Tectonostratigraphic synthesis and structural style of the Alborz mountain system in northern Iran. J Geodyn 21:1–33

Alizada A, Aliyeva E, Huseynov D, Guliyev I (2014) The Elemental stratigraphy of the South Caspian Lower Pliocene Productive series. In: STRATI 2013. Springer, Berlin, pp 827–831

Allen MB, Armstrong HA (2008) Arabia–Eurasia collision and the forcing of mid-Cenozoic global cooling. Palaeogeogr Palaeoclimatol Palaeoecol 265:52–58. https://doi.org/10.1016/j.palaeo.2008.04.021

Allen MB, Vincent SJ, Alsop GI, Ismail-zadeh A, Flecker R (2003a) Late Cenozoic deformation in the South Caspian region: effects of a rigid basement block within a collision zone. Tectonophysics 366:223–239

Allen MB, Ghassemi MR, Shahrabi M, Qorashi M (2003b) Accommodation of late Cenozoic oblique shortening in the Alborz range northern Iran. J Struct Geol 25:659–672

Allen MB, Jackson J, Walker R (2004) Late Cenozoic reorganization of the Arabia–Eurasia collision and the comparison of short-term and long-term deformation rates. Tectonics 23:TC2008

Allen MB, Blanc EJ-P, Walker R, Jackson J, Talebian M, Ghassemi MR (2006) Contrasting styles of convergence in the Arabia–Eurasia collision: why escape tectonics does not occur in Iran. Geol Soc Am Spec Pap 409:579–589

Allen MB, Kheirkhah M, Emami MH, Jones SJ (2011) Right-lateral shear across Iran and kinematic change in the Arabia–Eurasia collision zone. Geophys J Int 184:555–574. https://doi.org/10.1111/j.1365-246X.2010.04874.x

Axen GJ, Lam PS, Grove M, Stockli DF, Hassanzadeh J (2001) Exhumation of the west-central Alborz Mountains, Iran, Caspian subsidence, and collision-related tectonics. Geology 29:559–562

Bagirov E, Nadirov R, Lerche I (1997) Hydrocarbon evolution for a north–south section of the South Caspian Basin. Mar Pet Geol 14:773–854

Ballato P et al (2011) Arabia–Eurasia continental collision: insights from late Tertiary foreland-basin evolution in the Alborz Mountains northern Iran. GSA Bull 123:106–131

Ballato P et al (2013) Accommodation of transpressional strain in the Arabia–Eurasia collision zone: new constraints from (U–Th)/He thermochronology in the Alborz mountains north Iran. Tectonics 32:1–18

Berberian M (1983) The southern Caspian: a compressional depression floored by a trapped, modified oceanic crust. Can J Earth Sci 20:163–183

Berberian M, King G (1981) Towards a paleogeography and tectonic evolution of Iran. Can J Earth Sci 18:210–265

Berra F, Angiolini L (2014) The evolution of the Tethys region throughout the Phanerozoic: a brief tectonic reconstruction. In: Marlow L, Kendall C, Yose L (eds) Petroleum systems of the Tethyan region. AAPG Memoir, vol 106, pp 1–27

Berra F, Zanchi A, Mattei M, Nawab A (2007) Late Cretaceous transgression on a Cimmerian high (Neka Valley, Eastern Alborz, Iran): a geodynamic event recorded by glauconitic sands. Sed Geol 199:189–204. https://doi.org/10.1016/j.sedgeo.2007.02.001

Bretis B, Grasemann B, Conradi F (2012) An active fault zone in the western Kopeh Dagh (Iran). Aust J Earth Sci 105:3

Brunet M-F, Korotaev MV, Ershov AV, Nikishin AM (2003) The South Caspian Basin: a review of its evolution from subsidence modelling. Sed Geol 156(02):119–148. https://doi.org/10.1016/S0037-0738 00285–3

Brunet M-F, Ershov AV, Volozh YA, Korotaev MV, Antipov MP, Cadet J-P (2007) Precaspian and South Caspian Basins: subsidence evolution of two superdeep basins. in Yilmaz PO, Isaksen GH (eds), Oil and gas of the Greater Caspian area: AAPG studies in geology, vol 55, pp 151–155

Buryakovsky L, Aminzadeh F, Chilingarian G (2001) Petroleum geology of the south Caspian Basin. Gulf Professional Publishing, Houston

Cohen K, Finney S, Gibbard P, Fan J-X (2013) The ICS international chronostratigraphic chart. Episodes 36:199–204

Diaconescu CC, Kieckhefer R, Knapp J (2001) Geophysical evidence for gas hydrates in the deep water of the South Caspian Basin. Azerb Mar Pet Geol 18:209–221

Efendiyeva I (2000) Ecological problems of oil exploitation in the Caspian Sea area. J Pet Sci Eng 28:227–231

Fürsich FT, Wilmsen M, Seyed-Emami K, Majidifard MR (2009a) The Mid-Cimmerian tectonic event (Bajocian) in the Alborz Mountains, Northern Iran: evidence of the break-up unconformity of the South Caspian Basin. Geol Soc Lond Spec Publ 312:189–203. https://doi.org/10.1144/sp312.9

Fürsich FT, Wilmsen M, Seyed-Emami K, Majidifard MR (2009b) Lithostratigraphy of the Upper Triassic–Middle Jurassic Shemshak Group of Northern Iran. Geol Soc Lond Spec Publ 312:129–160. https://doi.org/10.1144/SP312.6

Ghorbani M (2013) The economic geology of Iran: mineral deposits and natural resources. Springer, Berlin

Golonka J (2007) Geodynamic evolution of the south Caspian Basin. In: Yilmaz PO, Isaksen GH (eds) Oil and gas of the Greater Caspian area. AAPG Stud Geol, vol 55, pp 17–41

Gorodnitskiy A, Brusilovskiy YV, Ivanenko A, Filin A, Shishkina N (2013) New methods for processing and interpreting marine magnetic anomalies: application to structure, oil and gas exploration, Kuril forearc, Barents Caspian seas. Geosci Front 4:73–85

Grasemann B, Wiesmayr G, Draganits E, Fusseis F (2004) Classification of refold structures. J Geol 112:119–125

Guest B, Axen GJ, Lam PS, Hassanzadeh J (2006a) Late Cenozoic shortening in the west-central Alborz Mountains, northern Iran, by combined conjugate strike-slip and thin-skinned deformation. Geosphere 2:35–52

Guest B, Stockli DF, Grove M, Axen GJ, Lam PS, Hassanzadeh J (2006b) Thermal histories from the central Alborz Mountains, northern Iran: implications for the spatial and temporal

distribution of deformation in northern Iran. Geol Soc Am Bull 118:1507–1521
Guliyev I, Mamedov P, Feyzullayev A, Huseynov D, Kadirov F, Aliyeva E, Tagiyev M (2003) Hydrocarbon systems of the South Caspian basin. Nafta-Press, Baku
Hadavi F, Moghaddam MN (2014) Nannostratigraphy, nannofossil events, and paleoclimate fluctuations in the lower boundary of Kalat formation in East KopetDagh (NE Iran). Arab J Geosci 7:1501–1515
Hollingsworth J, Jackson J, Walker R, Reza Gheitanchi M, Javad-Bolourchi M (2006) Strike-slip faulting, rotation, and along-strike elongation in the KopehDagh mountains, NE Iran. Geophys J Int 166:1161–1177. https://doi.org/10.1111/j.1365-246X.2006.02983.x
Hollingsworth J, Jackson J, Walker R, Nazari H (2008) Extrusion tectonics and subduction in the eastern South Caspian region since 10 Ma. Geology 36:763–766
Hollingsworth J et al (2010) Oroclinal bending, distributed thrust and strike-slip faulting, and the accommodation of Arabia–Eurasia convergence in NE Iran since the Oligocene. Geophys J Int 181:1214–1246
Jackson J, Priestley K, Allen M, Berberian M (2002) Active tectonics of the South Caspian Basin. Geophys J Int 148:214–245. https://doi.org/10.1046/j.1365-246X.2002.01588.x
Javanbakht M, Ghazi S, Moussavi-Harami R, Mahboubi A (2013) Depositional history and sequence stratigraphy of Tirgan formation (Barremian–Aptian) in central KopetDagh, NE Iran. J Geol Soc India 82:701–711
Jozanikohan G, Norouzi GH, Sahabi F, Memarian H, Moshiri B (2015) The application of multilayer perceptron neural network in volume of clay estimation: case study of Shurijeh gas reservoir, Northeastern Iran. J Nat Gas Sci Eng 22:119–131. https://doi.org/10.1016/j.jngse.2014.11.022
Kadirov F, Gadirov A (2014) A gravity model of the deep structure of South Caspian Basin along submeridional profile Alborz–Absheron Sill. Glob Planet Change 114:66–74
Katz B, Richards D, Long D, Lawrence W (2000) A new look at the components of the petroleum system of the South Caspian Basin. J Petrol Sci Eng 28:161–182
Kavoosi MA (2014) Inorganic control on original carbonate mineralogy and creation of gas reservoir of the Upper Jurassic carbonates in the Kopet–Dagh Basin, NE, Iran. Carbonates Evap 29:419–432
Kavoosi MA (2016) Depositional systems and sequence stratigraphy analysis of the Upper Callovian to Tithonian sediments in the Central and Western Kopet–Dagh Basin, Northeast Iran. Geol J 51:523–544
Kavoosi M, Lasemi Y, Sherkati S, Moussavi-Harami R (2009) Facies analysis and depositional sequences of the Upper Jurassic Mozduran Formation, a carbonate reservoir in the KopetDagh Basin, NE Iran. J Pet Geol 32:235–259
Knapp CC, Knapp JH, Connor JA (2004) Crustal-scale structure of the South Caspian Basin revealed by deep seismic reflection profiling. Mar Pet Geol 21:1073–1081
Lyberis N, Manby G, Poli J-T, Kalougin V, Yousouphocaev H, Ashirov T (1998) Post-Triassic evolution of the southern margin of the Turan plate ComptesRendus de l'Académie des Sciences-Series. IIA Earth Planet Sci 326:137–143
Mahboubi A, Moussavi-Harami R, Mansouri-Daneshvar P, Nadjafi M, Brenner RL (2006) Upper Maastrichtian depositional environments and sea-level history of the Kopet–Dagh intracontinental Basin, Kalat Formation. NE Iran Facies 52:237
Mattei M, Cifelli F, Muttoni G, Rashid H (2015) Post-Cimmerian (Jurassic–Cenozoic) paleogeography and vertical axis tectonic rotations of Central Iran and the Alborz Mountains. J Asian Earth Sci 102:92–101
Mattei M, Cifelli F, Alimohammadian H, Rashid H, Winkler A, Sagnotti L (2017) Oroclinal bending in the Alborz Mountains (Northern Iran): new constraints on the age of South Caspian subduction and extrusion tectonics. Gondwana Res 42:13–28
McQuarrie N, Stock J, Verdel C, Wernicke B (2003) Cenozoic evolution of Neotethys and implications for the causes of plate motions. Geophys Res Lett 30
Mousavi-Rouhbakhsh M (2001) Geology of the Caspian Sea Geological Survey of Iran, Tehran, rep **(in persian)**
Muttoni G et al (2009a) Opening of the Neo-Tethys Ocean and the Pangea B to Pangea A transformation during the Permian. GeoArabia 14:17–48
Muttoni G, Mattei M, Balini M, Zanchi A, Gaetani M, Berra F (2009b) The drift history of Iran from the Ordovician to the Triassic. Geol Soc Lond Spec Publ 312:7–29
Nabavi ST, Rahimi-Chakdel A, Khademi M (2017) Structural pattern and emplacement mechanism of the Neka Valley nappe complex, eastern Alborz, Iran. Int J Earth Sci 106:2387–2405
Narimanov A (1993) The petroleum systems of the South Caspian Basin. Basin Model Adv Appl Norwegian Pet Soc Spec Publ 3:599–608
Poursoltani MR, Gibling MR (2011) Composition, porosity, and reservoir potential of the Middle Jurassic Kashafrud Formation, northeast Iran. Mar Pet Geol 28:1094–1110
Rad FK (1982) Hydrocarbon potential of the eastern Alborz Region, NE Iran. J Pet Geol 4:419–435. https://doi.org/10.1111/j.1747-5457.1982.tb00552.x
Rad FK (1986) A Jurassic delta in the eastern Alborz, NE Iran. J Pet Geol 9:281–294. https://doi.org/10.1111/j.1747-5457.1986.tb00390.x
Raisossadat SN (2006) The ammonite family Parahoplitidae in the Sanganeh Formation of the KopetDagh Basin, north-eastern Iran. Cretac Res 27:907–922
Raisossadat N, Moussavi-Harami R (2000) Lithostratigraphic and facies analyses of the Sarcheshmeh Formation (Lower Cretaceous) in the eastern KopetDagh Basin, NE Iran. Cretac Res 21:507–516
Ramsay JG (1962) Interference patterns produced by the superposition of folds of similar type. J Geol 70:466–481
Rezaeian M, Carter A, Hovius N, Allen MB (2012) Cenozoic exhumation history of the Alborz Mountains, Iran: new constraints from low-temperature chronometry. Tectonics 31:TC2004. https://doi.org/10.1029/2011TC002974
Ritz J-F, Nazari H, Ghassemi A, Salamati R, Shafei A, Solaymani S, Vernant P (2006) Active transtension inside central Alborz: a new insight into northern Iran–southern Caspian geodynamics. Geology 34:477–480
Robert AMM, Letouzey J, Kavoosi MA, Sherkati S, Müller C, Vergés J, Aghababaei A (2014) Structural evolution of the KopehDagh fold-and-thrust belt (NE Iran) and interactions with the South Caspian Sea Basin and Amu Darya Basin. Mar Pet Geol 57:68–87. https://doi.org/10.1016/j.marpetgeo.2014.05.002
Seyed-Emami K (1975) Jurassic–Cretaceous Boundary in Iran. AAPG Bull 59:231–238
Seyed-Emami K, Fürsich FT, Wilmsen M (2004) Documentation and significance of tectonic events in the northern Tabas Block (east-central Iran) during the Middle and Late Jurassic. Res Paleontol Stratigr 2004:110
Smith-Rouch LS (2006) Oligocene–Miocene Maykop/Diatom total petroleum system of the South Caspian Basin Province, Azerbaijan, Iran, and Turkmenistan. US Geol Surv Bull 2201:1
Stampfli G, Marcoux J, Baud A (1991) Tethyan margins in space and time. Palaeogeogr Palaeoclimatol Palaeoecol 87:373–409
Stocklin J (1968) Structural history and tectonics of Iran, a review. AAPG Bull 52:1229–1258
Stöcklin J (1974) Possible ancient continental margins in Iran. In: The geology of continental margins. Springer, Berlin, pp 873–887

Taheri J, Fürsich FT, Wilmsen M (2009) Stratigraphy, depositional environments and geodynamic significance of the Upper Bajocian–BathonianKashafrud Formation, NE Iran. Geol Soc Lond Spec Publ 312:205–218. https://doi.org/10.1144/sp312.10

Tolosa I, de Mora S, Sheikholeslami MR, Villeneuve J-P, Bartocci J, Cattini C (2004) Aliphatic and aromatic hydrocarbons in coastal Caspian Sea sediments. Mar Pollut Bull 48:44–60

Torres MA (2007) The petroleum geology of Western Turkmenistan: the Gograndag–Okarem province. In: Yilmaz PO, Isaksen GH (eds) Oil and gas of the Greater Caspian area. AAPG studies in geology, vol 55, pp 109–132

Ulmishek GF (2001) Petroleum geology and resources of the North Caspian Basin, Kazakhstan and Russia. US Department of the Interior, US Geological Survey

Vernant P et al (2004) Deciphering oblique shortening of central Alborz in Iran using geodetic data. Earth Planet Sci Lett 223:177–185

Vincent SJ, Allen MB, Ismail-Zadeh AD, Flecker R, Foland KA, Simmons MD (2005) Insights from the Talysh of Azerbaijan into the Paleogene evolution of the South Caspian region. Geol Soc Am Bull 117:1513–1533. https://doi.org/10.1130/B25690.1

Zanchetta S, Berra F, Zanchi A, Bergomi M, Caridroit M, Nicora A, Heidarzadeh G (2013) The record of the Late Palaeozoic active margin of the Palaeotethys in NE Iran: constraints on the Cimmerian orogeny. Gondwana Res 24:1237–1266. https://doi.org/10.1016/j.gr.2013.02.013

Zanchi A, Berra F, Mattei M, Ghassemi MR, Sabouri J (2006) Inversion tectonics in central Alborz, Iran. J Struct Geol 28:2023–2037

Zanchi A, Zanchetta S, Berra F, Mattei M, Garzanti E, Molyneux S, Nawab A, Sabouri J (2009) The Eo-Cimmerian (Late? Triassic) orogeny in North Iran. Geol Soc Lond Spec Publ 312:31–55

Zanchi A, Zanchetta S, Balini M, Ghassemi MR (2016) Oblique convergence during the Cimmerian collision: evidence from the Triassic Aghdarband Basin, NE Iran. Gondwana Res 38:149–170. https://doi.org/10.1016/j.gr.2015.11.008